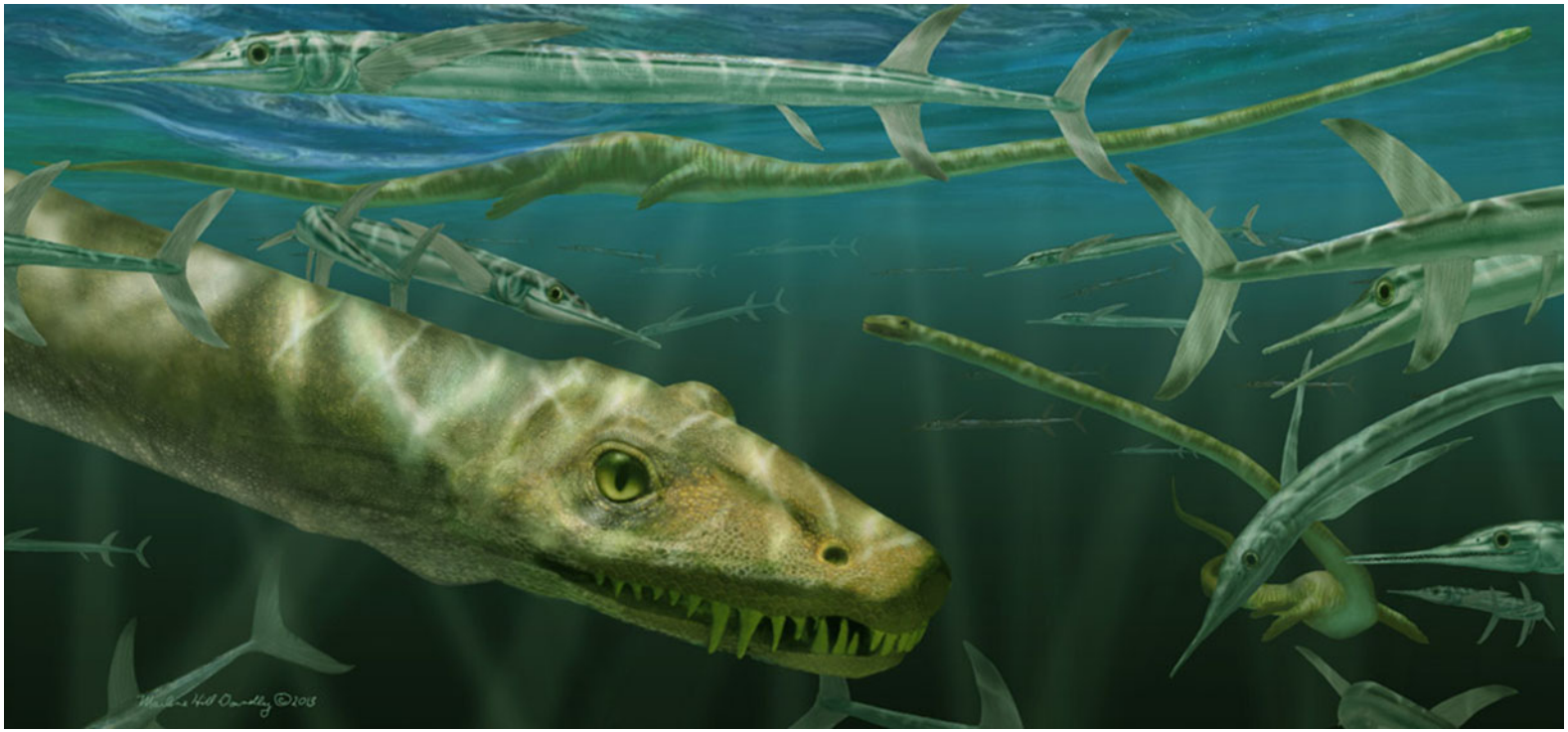

Frontispiece Restoration of *Dinocephalosaurus orientalis* depicted among a shoal of the large, predatory actinopterygian fish, *Saurichthys*. Artwork copyright Marlene Donnelly.

Earth and Environmental Science Transactions of the Royal Society of Edinburgh, **114**, 218–250, 2023 (for 2024)

Spontaneous Article

Dinocephalosaurus orientalis Li, 2003: a remarkable marine archosauromorph from the Middle Triassic of southwestern China

Stephan N.F. SPIEKMAN[1], Wei WANG[2], Lijun ZHAO[3], Olivier RIEPPEL[4], Nicholas C. FRASER[5]* and Chun LI[2]*

[1] Staatliches Museum für Naturkunde Stuttgart, Rosenstein 1, 10191 Stuttgart, Germany.
[2] Key Laboratory of Vertebrate Evolution and Human Origins of the Chinese Academy of Sciences, Institute of Vertebrate Palaeontology and Palaeoanthropology, Beijing 100044, China.
[3] Zhejiang Museum of Natural History, 310014, Hangzhou, China.
[4] The Field Museum of Natural History, 1400 Lake Shore Drive, Chicago, IL 60605, USA.
[5] National Museums Scotland, Chambers Street, Edinburgh EH1 1 JF, UK.
*Corresponding author. Email: lichun@ivpp.ac.cn; nick.fraser@nms.ac.uk

ABSTRACT: The non-archosauriform archosauromorph *Dinocephalosaurus orientalis* was first described from the Upper Member of the Guanling Formation (late Anisian, Middle Triassic) of Guizhou Province by Li in 2003 on the basis of a complete articulated skull and the first three cervical vertebrae exposed in dorsal to right lateral view. Since then, additional specimens have been discovered in southwestern China. Here, five newly discovered specimens are described for the first time, and redescriptions of the holotype IVPP V13767 and another referred specimen, IVPP V13898, are provided. Together, these permit the description of the complete skeleton of this remarkable long-necked marine reptile. The postcranial skeleton is as much as 6 metres long, and characterised by its long tail and even longer neck. The appendicular skeleton exhibits a high degree of skeletal paedomorphosis recalling that of many sauropterygians, but the skull and neck are completely inconsistent with sauropterygian affinities. The palate does not extend back over the basisphenoid region and lacks any development of the closed condition typical of sauropterygians. The arrangement of cranial elements, including the presence of narial fossae, is very similar to that seen in another long-necked archosauromorph, *Tanystropheus hydroides*, which at least in part represents a convergence related to an aquatic piscivorous lifestyle. The long and low cervical vertebrae support exceptionally elongate cervical ribs that extend across multiple intervertebral joints and contribute to a 'stiffening bundle of ribs' extending along the entire ventral side of the neck, as in many other non-crocopodan archosauromorphs. The functional significance of the extraordinarily elongate neck is hard to discern but it presumably played a key role in feeding, and it is probably analogous to the elongate necks seen in pelagic, long-necked plesiosaurs. *Dinocephalosaurus orientalis* was almost certainly a fully marine reptile and even gave birth at sea.

KEY WORDS: late Anisian, marine reptile, non-archosauriform, southern China.

Introduction

Archosauromorpha first appeared in the Permian and subsequently radiated into one of the dominant terrestrial vertebrate groups of the Mesozoic following the end-Permian mass extinction event (Ezcurra *et al.* 2014). Although most research has focussed on the radiation of crown archosaurs, the pseudosuchian or croc-line archosaurs and the avemetatarsalian or bird-line archosaurs, respectively (e.g., Brusatte *et al.* 2010; Langer *et al.* 2010; Butler *et al.* 2011; Nesbitt 2011), the earliest branching archosaurs or non-archosauriform archosauromorphs achieved remarkably high diversity and represented important components of both terrestrial and aquatic ecosystems during the Triassic (Foth *et al.* 2016; Ezcurra & Butler 2018; Spiekman *et al.* 2021). This group consists, among others, of the robust and herbivorous Rhynchosauria and Allokotosauria, as well as the more gracile *Protorosaurus speneri*, *Prolacerta broomi*, and long-necked Tanystropheidae. These gracile forms were previously considered to represent a monophyletic clade, 'Protorosauria', but several independent phylogenetic analyses have since revealed this to represent a para- or polyphyletic grouping, depending on the placement of *Prolacerta broomi* (e.g., Pritchard *et al.* 2015; Ezcurra 2016; Spiekman *et al.* 2021). Instead, these taxa can be

 doi:10.1017/S175569102400001X

described as non-crocopodan archosauromorphs, since Crocopoda comprises all archosauromorphs more closely related to allokotosaurs, rhynchosaurs and archosauriforms than to *Protorosaurus speneri* and tanystropheids (Ezcurra 2016).

The occurrence of terrestrial (e.g., *Macrocnemus bassanii*), aquatic (*Tanytrachelos ahynis* [freshwater] and *Tanystropheus hydroides* [marine]) and possibly even gliding forms (*Ozimek volans*) with widely different postcranial proportions and dental configuration suggests that non-crocopodan archosauromorphs, and in particular the tanystropheids, were highly diverse during the Triassic (Dzik & Sulej 2016; Spiekman *et al*. 2020a, 2021). Our understanding of these forms has been quite restricted due to the generally poor (highly compressed) and fragmentary preservation of specimens, particularly when compared with the largely complete and generally three-dimensionally preserved skulls known from other early archosauromorphs. However, the recent descriptions of *Tanystropheus hydroides* (Spiekman *et al*. 2020a, 2020b) and *Macrocnemus bassanii* (Miedema *et al*. 2020) aided by high resolution μCT data have provided much-needed insights into the three-dimensional cranial anatomy of key taxa. Nevertheless, additional relatively complete and three-dimensionally preserved fossils of other taxa are still required to allow us to appreciate the anatomical and ecological disparity of the group. In the last twenty years, new discoveries from the Middle Triassic of China have yielded a remarkable array of non-crocopodan archosauromorphs that either represent tanystropheids or closely related taxa. These include the highly gracile *Pectodens zhenyuensis* (Li *et al*. 2017b) and the long-necked and long-snouted *Fuyuansaurus acutirostris* (Fraser *et al*. 2013), both of which are known from relatively complete skeletons. Remains of *Macrocnemus* and *Tanystropheus* from China also suggest close ties between both aquatic and terrestrial faunas from the western and eastern Tethys provinces (Li 2007; Rieppel *et al*. 2010; Scheyer *et al*. 2020). However, the most remarkable among these new discoveries has been *Dinocephalosaurus orientalis*.

The original description of *Dinocephalosaurus orientalis* was based on an isolated well-preserved skull and the first three anterior cervical vertebrae preserved in articulation, and it was identified as a 'protorosaur' (Li 2003). Further specimens revealed that *Dinocephalosaurus orientalis* had a very similar size to *Tanystropheus hydroides* with comparable body proportions, including an extremely long neck, in addition to a very similar type of dentition. However, the paddle-shaped autopodia and much reduced carpal and tarsal bones in *Dinocephalosaurus orientalis* contrast sharply with the limb elements of *Tanystropheus* spp. and other non-crocopodan archosauromorphs. Furthermore, in contrast to the highly elongated neck of *Tanystropheus hydroides* and *Tanystropheus longobardicus*, composed only of 13 hyper-elongate cervical vertebrae, the neck of *Dinocephalosaurus orientalis* was found to consist of at least 32 vertebrae, suggesting that both genera had achieved their comparable neck elongation independently (Li *et al*. 2004; Nosotti 2007; Rieppel *et al*. 2008; Rieppel *et al*. 2010). The degree of adaptation to a marine lifestyle has additionally been highlighted by the discovery of two separate embryos, referable to *Dinocephalosaurus* sp. (Liu *et al*. 2017) and a separate closely related, but unnamed, taxon (Li *et al*. 2017a), respectively. The former occurs in the abdominal region of a partially articulated specimen, while the latter is an isolated, curled-up, complete skeleton. Both originate from Luoping County (Yunnan Province) as opposed to Guizhou Province, where the primary *Dinocephalosaurus orientalis* specimens were discovered. Together, these two records provided the first evidence of viviparity in the archosauromorph lineage. Although viviparity has also been established in terrestrial lepidosaurs (i.e., in some snakes and squamates), it is likely to represent an important adaptation for certain secondarily aquatic tetrapods, as it foregoes the need to venture on land to lay eggs. A recent revision of the phylogeny of non-crocopodan archosauromorphs (i.e., the former 'Protorosauria'), recovered *Dinocephalosaurus orientalis* in a clade with *Pectodens zhenyuensis*, dubbed Dinocephalosauridae, which formed the sister clade to Tanystropheidae (Spiekman *et al*. 2021). This result corroborates the convergent acquisition of aquatic adaptations and neck elongation that was previously discussed (Li *et al*. 2004; Rieppel *et al*. 2008) between *Dinocephalosaurus orientalis* and *Tanystropheus* spp., providing further evidence of the high diversity of Triassic non-archosauriform archosauromorphs.

The holotype specimen of *Dinocephalosaurus orientalis* (Institute of Vertebrate Paleontology and Paleoanthropology, Beijing, IVPP V13767) was collected near Xinmin in Panxian County, southwestern Guizhou Province. It came from the Upper Member of the Guanling Formation, which is of Pelsonian (late Anisian, Middle Triassic) age as indicated by the conodont *Nicoraella kockeli* (Sun *et al*. 2006, 2009; Zhang *et al*. 2009). This stratum has yielded a rich assemblage of marine reptiles, in particular numerous ichthyosaurs and sauropterygians, as well as fishes (Jiang *et al*. 2003, 2005a, 2005b, 2006a, 2006b, 2007, 2008; Li *et al*. 2006; Shang 2006; Motani *et al*. 2008). *Dinocephalosaurus orientalis* is not a common member of this assemblage, but since the discovery of the holotype a number of additional specimens have come to light. The first of these (referred specimen, IVPP V13898; Li *et al*. 2004; Rieppel *et al*. 2008), a nearly complete but partially disarticulated skeleton with the tail missing, has been described previously, and was the first specimen to reveal much of the postcranium. The skull in this specimen is strongly dorsoventrally compressed and exposed in ventral view only. Another specimen, this time from Luoping County, has been described (Liu *et al*. 2017) with associated embryonic remains (see above). Preserving fragmentary cranial remains, as well as part of the neck, thorax, tail and hindlimbs, it was referred to the genus *Dinocephalosaurus* (Liu *et al*. 2017), but the authors deferred from assigning it to a species. In recent years, five additional specimens have been collected from the type locality, which are housed either at the Institute of Vertebrate Paleontology and Paleoanthropology, Beijing (IVPP), or at the Zhejiang Museum of Natural History, Hangzhou (ZMNH). Here, we provide a detailed description of the skeletal anatomy of this new material, including comparisons to other non-crocopodan archosauromorphs, and a phylogenetic revision of the taxon. Due to the excellent preservation of the material, which includes relatively undistorted material and articulated remains, *Dinocephalosaurus orientalis* now represents one of the best-known non-crocopodan archosauromorphs.

1. Systematic palaeontology

Diapsida Osborn 1903
Archosauromorpha von Huene 1946
Dinocephalosauridae Spiekman *et al*. 2021
Dinocephalosaurus Li 2003.

Type species: *Dinocephalosaurus orientalis* Li 2003.

Diagnosis: as for the type species, the only known species in this genus.

Distribution: Upper Member of the Guanling Formation (late Anisian, Middle Triassic) near Xinmin in Panxian County, southwestern Guizhou Province, and in Luoping County, eastern Yunnan Province, P.R. China.

Dinocephalosaurus orientalis Li 2003

Holotype: Institute of Vertebrate Paleontology and Paleoanthropology, Beijing, IVPP V13767; skull and lower jaw exposed in right laterodorsal view; atlas, axis and partial third cervical vertebra; fragments of anterior cervical ribs.

https://doi.org/10.1017/S175569102400001X

Referred specimens: IVPP V13898: nearly complete but partially disarticulated skeleton, tail missing; IVPP V17977: skull and mandible exposed in ventral view, in articulation with 16 cervical vertebrae; IVPP V20295: the most complete specimen with skull exposed in dorsal view and the neck and body coiled around each other and the entire tail preserved; ZMNH M8727: partially preserved skull, neck and anterior trunk with forelimbs; ZMNH M8728: partially preserved skull, neck and anterior trunk with forelimbs; ZMNH M8752: complete skeleton (skull badly crushed).

Emended diagnosis: A non-crocopodan archosauromorph of relatively large size (up to 6 metres in total body length) diagnosed by the following unique combination of characters (* indicates autapomorphies among non-archosauriform archosauromorphs): neck that is more than twice as long as the trunk; skull with short postorbital region; antorbital recess distinct with external naris located in its anterior corner; jugal without posterior process; quadratojugal absent*; suborbital fenestra obliterated; interpterygoid vacuity very short and narrow, nearly completely obliterated; pterygoid separates palatine from vomer*; retroarticular process on lower jaw strongly reduced; a single premaxillary fang present; anterior maxillary and dentary fangs present; palatal dentition absent on at least the vomer and pterygoid*; 62 presacral vertebrae (32 cervical vertebrae), two sacral vertebrae and 81 caudal vertebrae; cervical vertebrae without hollow centrum and a neural spine with an anterodorsal anterior projection and posterodorsal posterior projection; vertebral centra constricted (ventral margin concave in lateral view), weakly amphicoelous; cervical ribs long and slender, aligned along neck and bridging from two to three (anterior neck) to five (middle neck) to six (posterior neck) intervertebral joints; cervical ribs with an elongate free-ending anterior process that extends considerably anteriorly beyond the prezygapophyses of the corresponding vertebra; sacral ribs not fused with corresponding vertebrae; absence of an ossified interclavicle; ilium lacking a preacetabular process but with a distinct dorsal iliac blade; thyroid fenestra absent; limbs relatively short and stout; stylopodium and zeugopodium of hindlimb somewhat shorter than of forelimb*; six carpal elements ossified; three tarsal elements ossified*; phalangeal count in manus reduced due to skeletal paedomorphosis*; no sutural contact between astragalus and calcaneum*; fifth metatarsal straight.

Type locality: Xinmin, Panxian County, Guizhou Province, southwestern China.

Horizon: Upper Member of Guanling Formation, Pelsonian, Anisian, Middle Triassic.

Ontogenetic assessment: LPV 30280 represents a gravid female and is thus sexually mature (Liu *et al*. 2017). Although this specimen currently cannot unambiguously be assigned to *Dinocephalosaurus orientalis*, it is referred to the same genus and was certainly closely related to the type species. Since this individual is smaller than all known specimens of *Dinocephalosaurus orientalis*, it can reasonably be ascertained that these also represented sexually mature individuals. The postcranium is poorly ossified in these specimens, but this is attributable to paedomorphosis related to aquatic adaptation, rather than skeletal immaturity.

2. Description

2.1. Holotype, specimen IVPP V13767

The holotype (Fig. 1) has been described by Li (2003), and again by Rieppel *et al*. (2008). It is represented by the skull and the right mandibular ramus exposed in right dorsolateral view, associated with the first three cervical vertebrae and the respective cervical ribs. It is the best-preserved skull amongst all the material, although it does not expose the dermal palate (which is beautifully exposed in IVPP V17977; see below). Unfortunately, sutural detail is frequently difficult to establish, possibly due to diagenesis. One of the most difficult regions to differentiate is the postorbital bar and the delimitation of the jugal, squamosal and postorbital. Li (2003) illustrated a pronounced dorsal process of the jugal separating the squamosal from the postorbital. However, a reinterpretation of the holotype by Rieppel *et al*. (2008) found that this region, which forms the posterior margin of the orbit, is formed by a prominent triradiate postorbital and that the jugal consequently did not reach as far dorsally as inferred by Li (2003). The element indicated as the postorbital by Li (2003) was instead found to be part of the postfrontal, which consequently forms a prominent, elongated element that is oriented transversely relative to the long axis of the skull. As such, the postfrontal forms the posterodorsal margin of the orbit and much of the anterior margin of the supratemporal fenestra. The interpretation by Rieppel *et al*. (2008) is corroborated here based on observations on IVPP V20295 (see below). However, the exact sutural contact between the squamosal, postorbital and jugal remains uncertain because the sutures between these elements have been obliterated in IVPP V13767 and because this region is badly broken in IVPP V20295. The holotype confirms the diapsid affinities of the taxon, with a lower temporal arch that remains incomplete (the quadratojugal is missing and was almost certainly absent, since it is not present in any of the well-preserved, articulated skulls). IVPP V13767 represents the largest known skull of *Dinocephalosaurus orientalis* and has a total length of 230 mm. The largest preserved tooth measures 28 mm from the base of the crown to the tip.

The holotype displays the highly characteristic dentition of the species, with a single premaxillary and two maxillary fangs. Three, possibly four, mandibular fangs fit in between the premaxillary and maxillary fangs when the jaws are closed. Equally characteristic of the species, and similar to the condition seen in *Tanystropheus hydroides* (Spiekman *et al*. 2020a, 2020b), is a distinct antorbital depression or recess that extends along the rostrum in front of the orbit. The external nares are positioned very close to the end of the rostrum, resembling the condition of *Pectodens zhenyuensis* (Li *et al*. 2017b). The lower jaw reveals a weakly developed coronoid process, and the reduction of the retroarticular process which – together with the weak posterior concavity of the quadrate – indicates the absence of a well-developed tympanic membrane in this marine organism.

2.2. Referred specimen, IVPP V13898

(Figure 2). IVPP V13898, which was described in detail by Rieppel *et al*. (2008; see also Li *et al*. 2004), comprises the skull, most of the vertebral column, elements of all four limbs and some elements of the pectoral and pelvic girdle (Fig. 2). The skull is relatively poorly preserved, strongly dorsoventrally compressed and exposed in ventral view. The cervical vertebral column is broken near the middle of the neck and again more posteriorly. The posterior trunk is represented by an incomplete string of vertebrae that curls around the remaining, partially disarticulated, trunk skeleton. The left fore- and hindlimbs are beautifully exposed and preserved in articulation. The right fore- and hindlimbs are partially obscured by ribs and elements of the remaining appendicular skeleton. The tail is missing.

The new material of *Dinocephalosaurus orientalis* that came to light after the description of IVPP V13898 (Li *et al*. 2004; Rieppel *et al*. 2008) clarified many details of the skeletal anatomy of this taxon, especially with respect to the vertebral column, which remained ambiguous on the basis of information gleaned from IVPP V13898 alone. This prompted us to reinvestigate the latter specimen in the light of the new discoveries.

2.2.1. The skull. The skull is preserved in palatal view and the palate is rather badly crushed so that no sutures can reliably be distinguished. Nevertheless, certain details, particularly on

https://doi.org/10.1017/S175569102400001X

Figure 1 The holotype of *Dinocephalosaurus orientalis* Li, 2003. (a) Photograph. (b) Photograph with interpretative drawing. Abbreviations: fr = frontal; j = jugal; la = lacrimal; mx = maxilla; na = nasal; op = opisthotic; pa = parietal; pl = palatine; pm = premaxilla; pof = postfrontal; po = postorbital; pro = prootic; pt = pterygoid; scl = sclerotic plates; soc = supraoccipital; sq = squamosal.

the right side, can be determined. For example, the contact between the maxilla and palatine is quite well exposed but there is no evidence of a suborbital fenestra. More anteriorly there is a narrow opening in the palate that we interpret as the posterior end of the right internal naris. Also, on the right side, the transverse process of the pterygoid, which would have articulated with, and ventrally overlapped, the ectopterygoid, is visible. It is characterised by a well-defined ridge that curves anterolaterally from the margin of the interpterygoid vacuity, but there is clearly no development of any ventrally directed pterygoid-ectopterygoid flange. This is a feature that is preserved even more clearly in IVPP V17977 (see below). Rieppel *et al.* (2008) postulated that the pterygoids met posteriorly along the midline and possibly even covered the basicranium. However, with the discovery of IVPP V17977, we now know that this is an artifact of preservation, and that the basioccipital and parabasisphenoid must be displaced in this specimen. The posterior end of the right mandibular ramus is well preserved and, as noted previously (Rieppel *et al.* 2008), supports earlier observations that the retroarticular process is considerably reduced in *Dinocephalosaurus orientalis.*

2.2.2. The cervical series. Behind the skull, the centrum of the atlas is preserved in direct articulation with the axis. As previously described (Rieppel *et al.* 2008), an additional 16 cervical vertebrae are articulated as a series behind the axis (making a total of 18 cervical vertebrae) before there is a clean break in the column. Following this an additional series of seven articulated cervical vertebrae extends at a right angle to the proximal 18 cervical vertebrae and in close association with a tight bundle of cervical ribs. It is not clear whether there are any cervical vertebrae missing at this first break in the axial skeleton, although it seems unlikely as there are no isolated sections of rib that cannot be matched with either of the two articulated sections.

https://doi.org/10.1017/S175569102400001X

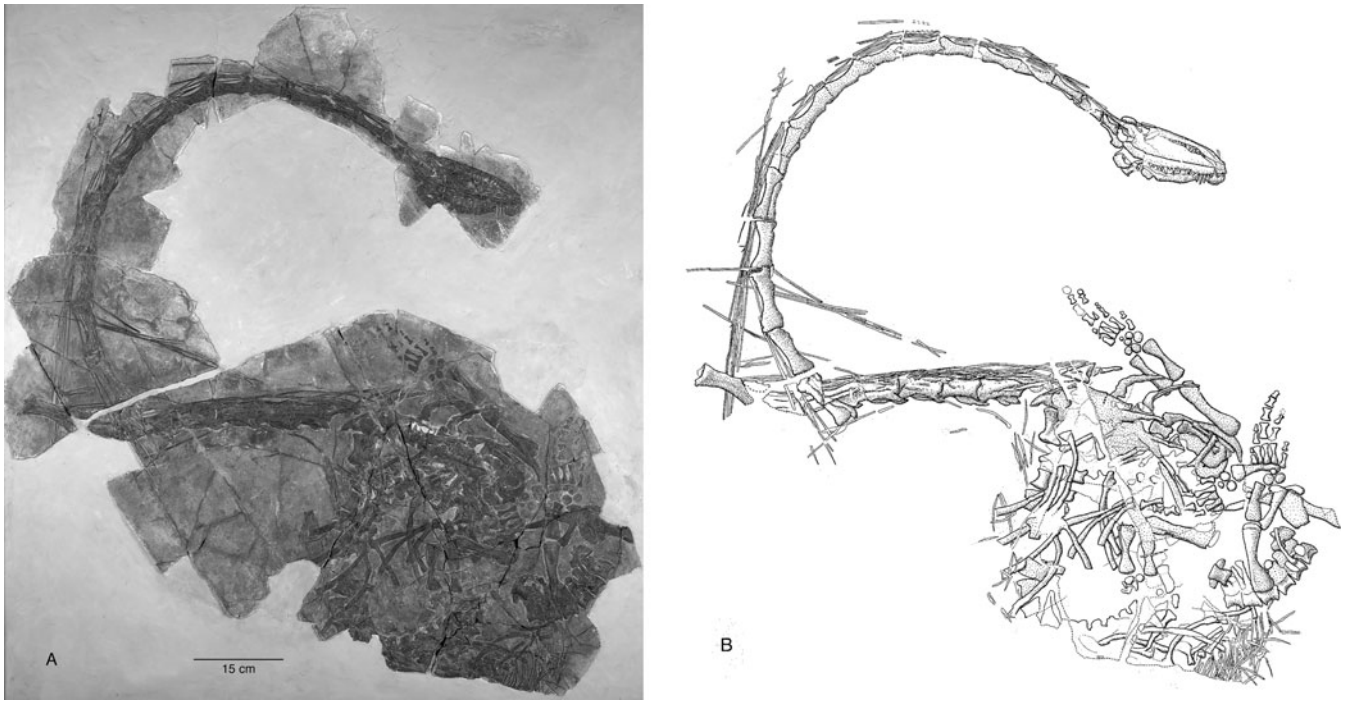

Figure 2 *Dinocephalosaurus orientalis*, IVPP V13898 (referred specimen). (a) Photograph. (b) Interpretative drawing, reproduced with permission of the Society of Vertebrate Paleontology.

There then follows a second break in the cervical column corresponding to a point between cervical 25 and 26. Here it appears that cervical 26 and 27 have been displaced and 'twisted' out of alignment with the rest of the column (Fig. 2) and are slightly disarticulated. Rieppel *et al*. (2008) were unable to come to any definitive conclusion on the number of cervical vertebrae, but based on a discernible reduction in length of the centra considered it most likely that the next vertebra in the series represented the first dorsal, despite the fact that the pectoral girdle is situated more posteriorly. However, we now know that in some long-necked early archosauromorphs, for example *Tanystropheus* spp., there is a distinct shortening of the most posterior cervical vertebrae compared to the anterior and mid cervical vertebrae. In this case the vertebrae can still be distinguished as cervical vertebrae based on their association with characteristic plough-shaped ribs (Rieppel *et al*. 2010), although those ribs are much shorter and more robust than the more anterior cervical ribs. Based on this knowledge it is now apparent that there are at least five additional vertebrae behind cervical 27 that are associated with shortened rather plough-shaped ribs with very robust heads. Thus, we consider this individual to show at least 32 cervical vertebrae. The ribs associated with vertebrae 28 and 29 have a clear anterior process, but this becomes less pronounced in the next three vertebrae. Nevertheless, they have greatly thickened heads that turn in sharply towards their articulations with the vertebrae. However, the exact distinction between the cervical and dorsal series remains somewhat equivocal as the region around the pectoral girdle is rather poorly preserved. Indeed, details of much of the trunk region, including the pectoral and pelvic girdles, are rather indistinct.

Rieppel *et al*. (2008) recorded the presence of the right ilium and pubis in fairly close association although not in complete articulation. The posterior edge of the pubis is relatively straight and lacks any posterior emargination. This is a condition that is confirmed by examination of ZMNH M8752 and IVPP V20295 (see below). *Dinocephalosaurus orientalis* therefore lacked a thyroid fenestra entirely. A thyroid fenestra is present in most tanystropheids, but it is absent in *Tanytrachelos ahynis* and *Fuyuansaurus acutirostris*, and in the probable non-tanystropheid archosauromorph *Jesairosaurus lehmani* (Spiekman *et al*. 2021). The ilium possesses a well-defined facet for the ischium set off from that for the pubis (Rieppel *et al*. 2008), but the ischium appears to be missing completely and therefore did not form a fused pubo-ischiadic plate with the pubis, similar to other early archosauromorphs. There may even have been a slight separation of the ischium and pubis along their ventral symphysis.

2.3. Referred specimen, IVPP V17977

(Figure 3). The specimen comprises the skull and mandible preserved in ventral view on one block, followed by the first to the 16th cervical vertebrae, together with associated cervical ribs, preserved in articulation on three additional slabs (Fig. 3). The skull measures 206 mm in length and 103 mm in width as preserved across the widest point of the skull.

2.3.1. The skull. The dermal palate is nearly closed in *Dinocephalosaurus orientalis*. Although beautifully exposed and lacking the level of crushing seen in IVPP V13898, it is still difficult to clarify details of the sutures, particularly between the palatines and the pterygoid. Some of the clearest are the interdigitating sutures separating the vomers from the pterygoids, and on the right side there appears to be a fairly well-defined suture between the palatine and vomer (Fig. 3b). Lateral to this suture, the posterior margin of the internal naris is clearly visible on the right side bounded by the palatine. A suborbital fenestra is absent, and the broad palatal rami of the pterygoids meet each other at the midline for most of their length. The contact between them is established shortly in front of the open palatobasal articulation. The palatal ramus of the pterygoid meets the ectopterygoid and palatine laterally and the broad vomer anteriorly, thus separating the paired palatines from each other along the midline. The very wide palatal ramus of the pterygoid resembles the condition seen in *Tanystropheus hydroides* (Spiekman *et al*. 2020b) and contrasts with the much narrower pterygoid seen in other tanystropheids and early archosauromorphs (e.g., *Macrocnemus* spp., Miedema *et al*. 2020; Scheyer *et al*. 2020, and *Azendohsaurus madagaskarensis*, Flynn *et al*. 2010). The boundaries between the palatines and pterygoids are completely indistinct. On the left side of the palate there is a prominent ridge running anteroposteriorly for at least two-thirds of the

https://doi.org/10.1017/S175569102400001X

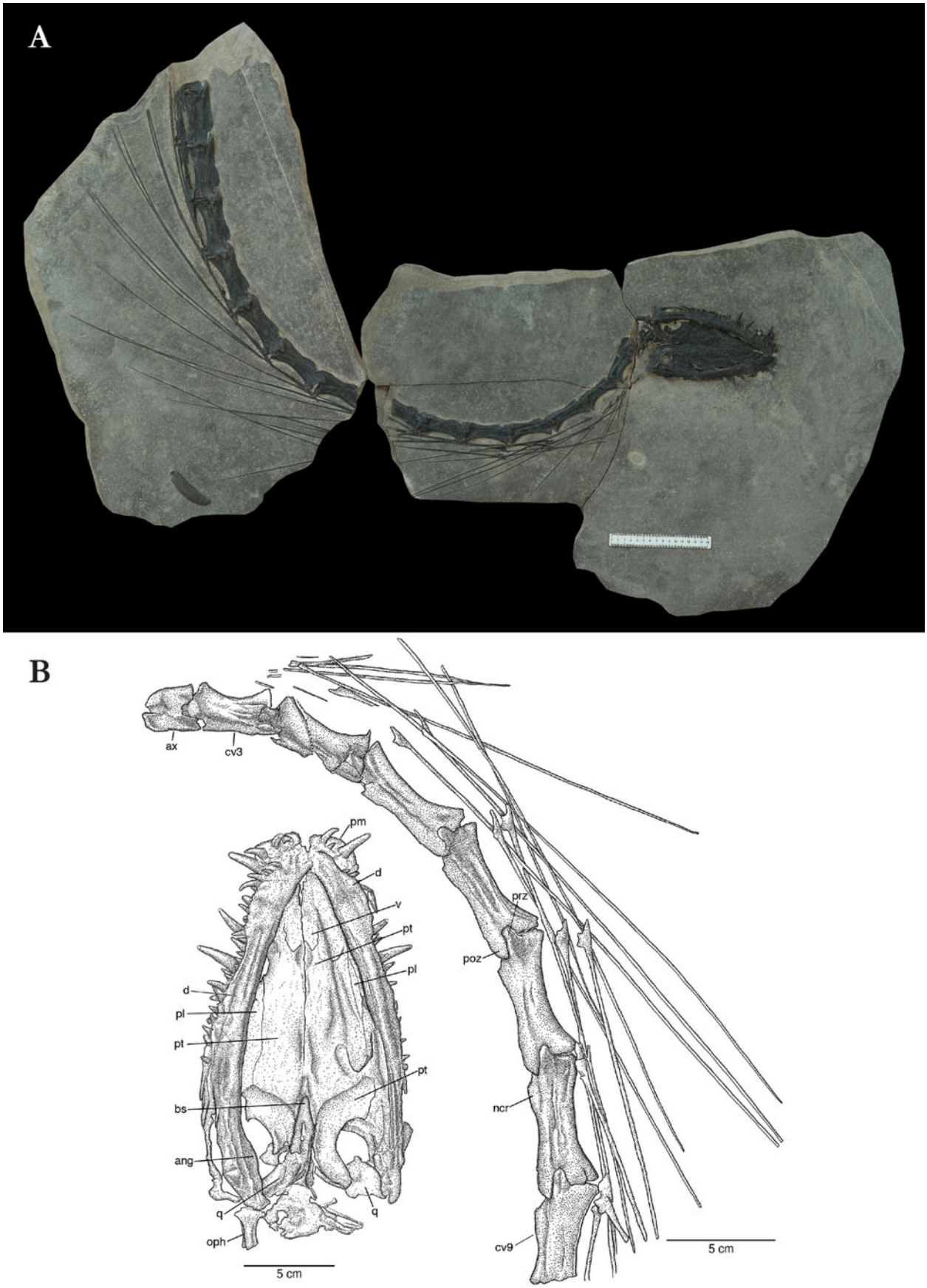

Figure 3 *Dinocephalosaurus orientalis*, IVPP V17977 (referred specimen). (a) The specimen as preserved on four slabs (photograph, scale bar in cm). (b) Interpretative drawing of the skull, lower jaw and cervical vertebrae 2–9. Abbreviations: ang = angular; ax = axis; bs = basisphenoid; cv = cervical vertebra; d = dentary; ncr = neural crest; oph = opisthotic; pl = palatine; poz = postzygapophysis; prz = prezygapophysis; pt = pterygoid; q = quadrate; v = vomer.

length of the entire palate (Fig. 3b). While superficially this appears to be an articulation between the two elements, significantly it is not repeated on the right side and it is completely inconsistent with the configuration of the palatine and pterygoid in other diapsids. A long connection with the palatine along the lateral margin of the palatal ramus of the pterygoid can also be observed in dorsal

https://doi.org/10.1017/S175569102400001X

view through the orbit in IVPP V20295 (see below). Therefore, the condition of the left side of the palate of IVPP V13898 is considered to be an artifact of preservation. Likewise, there is no obvious separation between the ectopterygoid and pterygoid. As noted above for IVPP V13898, there is a very clear ridge that essentially demarcates the anterior boundary of the pterygoid transverse process. This is preserved symmetrically on both sides but does not seem likely to represent the ectopterygoid-pterygoid boundary. Nor does it seem to represent an impression resulting from the extreme compression of the dorsal roof of the skull since its position is inconsistent with the position of either the orbital margins or the borders of the temporal fenestrae. We therefore regard this ridge as a characteristic feature of *Dinocephalosaurus orientalis*. The posterolateral corner of the transverse process of the pterygoid is curved posteriorly and hook-shaped in ventral view, which is a condition that is also found in *Jesairosaurus lehmani*, *Tanstropheus* spp., *Amotosaurus rotfeldensis* and certain allokotosaurs among early archosauromorphs (Spiekman *et al*. 2021). This posterior hook of the transverse flange of the pterygoid is absent in *Macrocnemus* spp. and *Prolacerta broomi*.

Although the palate would seem to be generally devoid of any dentition, there are the possible remnants of two small denticles preserved on what is taken to be the posterior edge of the right palatine just anterior to the transverse process of the pterygoid. Palatal dentition is present on the pterygoid, vomer and palatine in most non-archosauriform archosauromorphs in which these regions have been observed (Ezcurra 2016; Spiekman *et al*. 2021). However, *Tanystropheus hydroides* also shows a distinct reduction in palatal dentition, since it only possesses a single row of well-developed teeth along the outer margin of the vomer (Spiekman *et al*. 2020b).

The quadrate process of the pterygoid is broad and distinctly curved posterolaterally, its deeply concave lateral margin defining the medial contours of the relatively short subtemporal fenestra. The quadrate process of the pterygoid terminates in a blunt tip that contacts the medial aspect of the quadrate narrowly above its mandibular condyle.

Between the quadrate rami of the pterygoids the basicranium is exposed in ventral view. The ventral surface of the parabasisphenoid posterior to the palatobasal articulation is concave. Little morphological detail is discernible in the crushed bone that comprises the basioccipital, occipital condyle and the atlas centrum and neural arches. The first cervical ribs appear to have been articulating on the atlas. The right exoccipital and opisthotic are well preserved and exposed, however, indicating lack of fusion of these two elements. The exoccipital and opisthotic are generally not fused in mature specimens of non-archosauriform archosauromorphs, with the exception of *Tanystropheus hydroides* and certain allokotosaurs (Spiekman *et al*. 2021).

2.3.2. The mandible. The articulated mandible is exposed in ventral view. On the left mandibular ramus, a faint suture may represent the boundary of the splenial, but its boundaries remain unclear. In the right mandibular ramus, below the mandibular joint, the angular is exposed as a distinct medial expansion. The retroarticular process projects only slightly posterior to the glenoid fossa.

The broadened anterior tips of the premaxillaries protrude anteriorly from below the anterior ends of the dentaries. This condition is typical of *Dinocephalosaurus orientalis* among archosauromorphs, and can also be observed in the holotype skull. The right premaxilla shows that the fourth premaxillary tooth formed the enlarged premaxillary fang, as was also inferred to be the case in the holotype (Rieppel *et al*. 2008). On both sides, two enlarged maxillary fangs protrude from below the mandibular rami, separated from the premaxillary fang by a series of smaller teeth, the number of which cannot unequivocally be established. Indeed, the difficulty in unequivocally identifying maxillary versus dentary teeth, more numerously exposed on the right than on the left side, renders a precise tooth count for these two elements impossible. Those teeth lying immediately behind the right premaxillary fang belong to a well-defined series of anterior dentary teeth, which indicates the possible existence of a diastema in the upper jaw tooth row separating the premaxillary from the maxillary dentition. In the holotype skull, this diastema appears to accommodate two, possibly three, dentary teeth.

2.3.3. The vertebrae. The series of vertebrae are preserved with their right lateral sides exposed. The first nine elements are preserved in almost perfect articulation and even the cervical ribs are paired in relatively close association with their respective vertebrae, although they are splayed ventrally away from the long axis of the neck. There is then a short gap in the slab that accounts for the posterior part of the ninth vertebra together with all of the tenth vertebra. Vertebrae 11 to 17 are also preserved in perfect articulation with each other and their respective ribs. Each rib has a very distinctive anterior process that extends beyond the separate capitulum and tuberculum. In lateral view this anterior process has a distinct excavation on its dorsal edge just in front of the capitulum. The process then broadens out slightly before tapering again towards its anterior tip. This depression corresponds exactly to the position of the posterior edge of the preceding centrum and it seems likely that in life it formed a direct articulation with the centrum. If this was the case it might have permitted a certain degree of dorsiflexion of the neck. The relative length of the anterior process of the ribs is comparable to that seen in *Sclerostropheus fossai*, *Tanytrachelos ahynis* and *Pectodens zhenyuensis* among tanystropheids and dinocephalosaurids (Olsen 1979; Li *et al*. 2017b; Spiekman & Scheyer 2019) and also similar to that seen in the putative early archosauromorph *Czatkowiella harae* (Borsuk-Białynicka & Evans 2009), and considerably longer than that seen in other early archosauromorphs. The ribs on the first nine or ten vertebrae are almost entirely straight. But from cervical 11 onwards the ribs assume a very gentle uniform curvature. None exhibit the slight kinks described in the cervical ribs of a specimen of *Tanystropheus* (Rieppel *et al*. 2010) where they extended across the intervertebral joints.

2.4. Referred specimen, ZMNH M8727

(Figure 4). The exposed parts of the skeleton comprise elements of the exploded skull, a total of 28 cervical vertebrae of which the axis and the following 17 cervical vertebrae are preserved in articulation; two scattered vertebrae located next to the 28th cervical vertebra, one of them exposed in anterior view, represent shortened posterior cervical vertebrae. A string of six vertebrae lying in front of the remains of the pectoral girdle and forelimbs represent the posteriormost cervical and anteriormost dorsal vertebrae. Associated cervical, dorsal and gastral ribs are likewise exposed. The scattered remains of both pectoral girdles and forelimbs are also preserved (Fig. 4).

2.4.1. The skull and dentary. In the exploded skull the well-preserved right premaxilla (Fig. 5a) is exposed in medial view. The alveolar margin of the body of the premaxilla carries five identifiable tooth positions, of which the anteriormost and posteriormost ones are empty. The slender, tapering nasal process (prenarial process) of the premaxilla extends posterodorsally; its length is about twice that of the body of the premaxilla. This process would have separated the two external nares from each other, as is the case in most non-archosauriform archosauromorphs, except for *Tanystropheus* spp., certain allokotosaurs (e.g., *Shringasaurus indicus*, *Azendohsaurus madagaskarensis*, *Pamelaria dolichotrachela*), rhynchosaurs and *Teyujagua paradoxa*, in which the external nares are confluent (Dilkes 1998; Flynn *et al*. 2010; Pinheiro *et al*. 2019; Spiekman *et al*. 2020a, 2021). The process directed posteriorly from the main body of

https://doi.org/10.1017/S175569102400001X

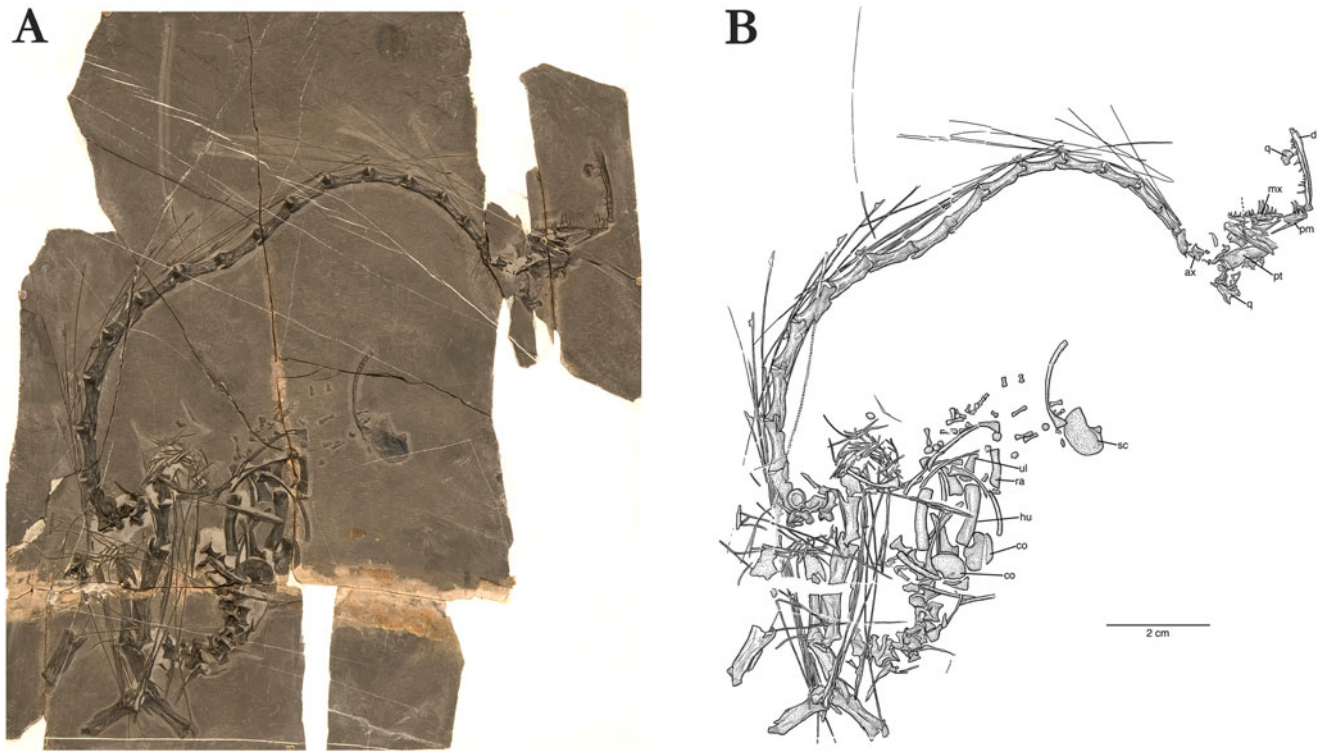

Figure 4 *Dinocephalosaurus orientalis*, ZMNH M8727 (referred specimen). (a) Photograph. (b) Interpretative drawing. Abbreviations: ax = axis; co = coracoid; d = dentary; hu = humerus; mx = maxilla; pm = premaxilla; pt = pterygoid; q = quadrate; ra = radius; sc = scapula; ul = ulna.

the premaxilla (postnarial process) is strongly reduced in *Dinocephalosaurus orientalis* and tapers posterodorsally. Three premaxillary teeth are preserved in the second to the fourth tooth positions. Tooth implantation (*sensu* Ezcurra 2016) is subthecodont. The third and fourth teeth are equal in length while distinctly longer than the second tooth. The teeth are pointed and recurved, and the enamel surface is distinctly striated in the apical part. Resorption pits are located on the labial side of the tooth base, with a replacement tooth located inside its pit at the base of the third premaxillary tooth.

Located behind the right premaxilla lies the right maxilla, which is also exposed in medial view (Fig. 5b). The maxilla carries a rather slender anterior process that projects beyond the anteriormost preserved tooth, and that ends in a blunt tip. Its

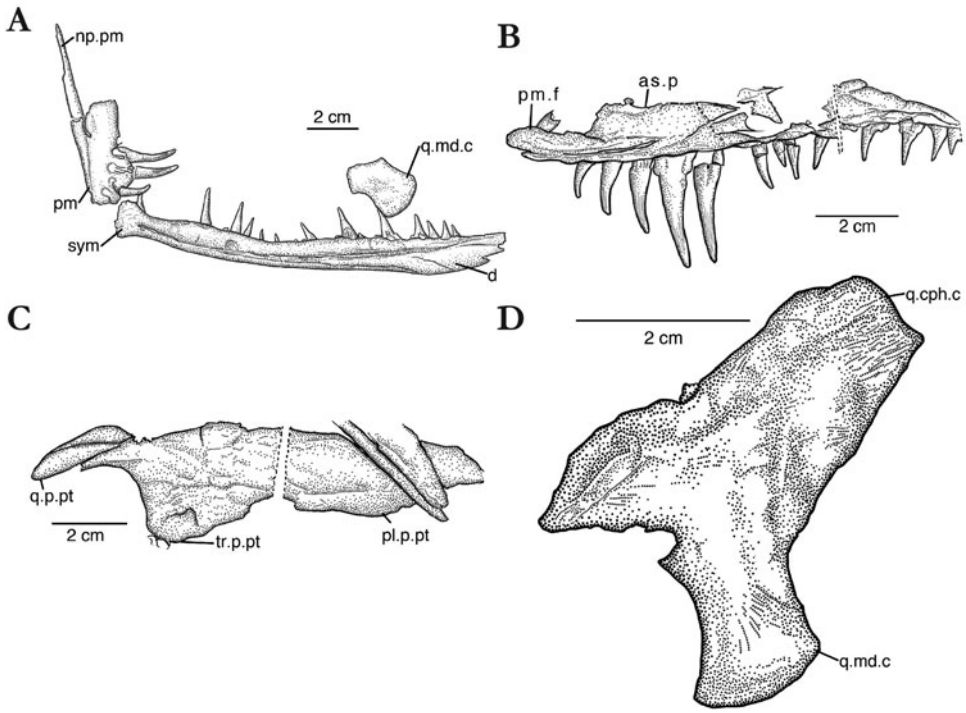

Figure 5 *Dinocephalosaurus orientalis*, ZMNH M8727, interpretative drawings of selected cranial remains. (a) Premaxilla, dentary and mandibular condyle of quadrate. (b) Right maxilla in medial view. (c) Left pterygoid in ventral view. (d) Right (?) quadrate in medial (?) view. Abbreviations: as.p = ascending process of the maxilla; d = dentary; np.pm = nasal process of the premaxilla; pl.p.pt = palatine process of the pterygoid; pm = premaxilla; pm.f = premaxillary process of the maxilla; q.cph.c = cephalic condyle of the quadrate; q.md.c = medial condyle of the quadrate; q.p.pt = quadrate process of the pterygoid; sym = symphysis; tr.p.pt = transverse process of the pterygoid.

https://doi.org/10.1017/S175569102400001X

dorsal margin would seem to have defined the lateral margin of the external naris that was located within the antorbital recess. The ascending (facial) process of the maxilla ascends rather abruptly at what appears to have been the level of the posterior margin of the external naris. From there, the dorsal margin of the ascending process gently curves posterodorsally, the maxilla thus gaining in height. The ascending process is damaged (incomplete) in its posterior part, which does not allow us to ascertain whether it defined the anterior margin of the orbit, or whether a lacrimal was present. Although again incomplete at its posterior end, the maxilla does show a tapering, tooth-bearing suborbital process extending posteriorly below the anterior part of the orbit, as is also seen in the skull of the holotype.

The holotype skull (Fig. 1) shows a minimum of three maxillary teeth preceding the paired maxillary fangs, and the same is observed in ZMNH M8727. If this is indeed the natural condition, the anterior process of the maxilla, lining the external naris laterally, would be edentulous and the premaxillary and maxillary tooth row would thus be separated by a diastema that accommodates anterior dentary teeth. The total number of teeth preserved on the left maxilla amounts to 13, to which may be added four, possibly five, empty tooth positions (the posterior tip of the maxilla is missing). Tooth implantation is thecodont (*sensu* Ezcurra 2016). The relatively long anterior maxillary teeth are distinctly recurved, the shorter posterior maxillary teeth are straight. All teeth are pointed, the enamel covering distinctly striated towards the apex of the crown. The base of the teeth reveals deep striations that appear to result from infolding, thus revealing the presence of plicidentine in *Dinocephalosaurus orientalis*. Plicidentine has previously not been established in any archosauromorph reptile, but is known to occur in ichthyosaurs, choristoderes, squamates and possibly sauropterygians among diapsids (Maxwell *et al*. 2011; Spiekman & Klein 2021). The morphology of the tooth crowns is very similar to that seen in *Tanystropheus hydroides* (Spiekman *et al*. 2020b). This taxon similarly possesses fang-like, striated maxillary teeth that are heterogeneous in size. In *Tanystropheus hydroides*, the maxillary teeth increase in size until tooth position seven, after which the size of the teeth gradually decreases until the 15th and terminal tooth position. However, in contrast to *Dinocephalosaurus orientalis*, tooth implantation in the maxilla of *Tanystropheus hydroides* is distinctly subthecodont and there is no plicidentine infolding at the tooth roots.

The parietal skull table is preserved in ventral view, pierced by the relatively large pineal foramen located well within the parietal. The posterolateral (supratemporal) processes of the parietal are incomplete, however. The irregularly shaped, but essentially triradiate element located next to the parietal skull table most likely represents a damaged, or incompletely exposed postorbital.

The left pterygoid is well exposed in ventral view (Fig. 5c). It shows the large, broad, plate-like palatal ramus, which, as mentioned above, is similar in outline to that of *Tanystropheus hydroides* (Spiekman *et al*. 2020b), and which dominates the formation of the nearly closed dermal palate. The transverse posterior margin that defines the anterior margin of the subtemporal fenestra is nearly straight. The relatively slender quadrate ramus of the pterygoid curves posterolaterally, forming a concave lateral margin. A distinct notch on the medial margin of the pterygoid, located at the juncture of the palatine and quadrate rami, marks the location of the palatobasal articulation. The anterior end of the palatal ramus of the left pterygoid is crossed over by the anterior end of the incompletely preserved palatal ramus of the right pterygoid, its posterior end broken.

Two ossifications are identifiable as representing the quadrates (Fig. 4b). One is located next to the disarticulated right dentary. It is a relatively small ossification of irregular pentagonal shape, its smoothly convex ventral margin forming the mandibular condyle. The other quadrate lies at some distance from the posterior end of the left pterygoid, again showing the same convex configuration of the mandibular condyle. In contrast to the (presumably) right quadrate, the (presumably) left quadrate is dorsally broadly expanded (Fig. 5d). It lacks the hook-shaped posterior end of the dorsal head seen in *Tanystropheus hydroides*, *Tanystropheus longobardicus* and allokotosaurs (Flynn *et al*. 2010; Spiekman *et al*. 2020b, 2021; Sengupta & Bandyopadhyay 2022). The posterior margin is distinctly concave due to a posterodorsal expansion that terminates in a pointed tip. Much more expansive is an anterodorsal, deep and flange-like expansion, forming what looks like an anterodorsal wing of the quadrate. By comparison to the holotype skull, it appears that the (presumably) left quadrate is associated with incomplete remains of the squamosal.

The right dentary is beautifully exposed in medial view (Fig. 5a). It is a slender element that is expanded at its anterior tip, forming a somewhat fortified mandibular symphysis, which is similar to the condition seen in *Tanystropheus hydroides*, albeit less strongly developed (Spiekman *et al*. 2020b). A distinct alveolar shelf overhangs Meckel's canal and carries the dentary teeth. Posteriorly, the dentary gains somewhat in depth, terminating in an indented convex margin. The indentations most probably accommodated the anterior tip of the surangular. A total of 13 complete teeth are preserved on the dentary, an incomplete number. The complete tooth count is difficult to estimate, but could comprise as many as 20 to 21 teeth. Tooth implantation is thecodont (*sensu* Ezcurra 2016). The teeth are pointed, covered with striated enamel apically, and showing indications of resorption pits and plicidentine infolding on the lingual aspect of the tooth base. The anteriormost preserved dentary tooth is distinctly recurved, but more anteriorly than in the upper tooth row the dentary teeth subsequently become upright.

2.4.2. The vertebral column. (Table 1). Two kidney-shaped ossifications located in front of the axis could represent the atlas neural arches. The axis is disarticulated but aligned with the cervical series behind it and it is beautifully exposed in left lateral view (Fig. 6a). It is distinctly shorter than the third and subsequent cervical vertebrae. The ventral margin of the centrum is strongly concave in lateral view. At the anterior end of the centrum the pedicel of the neural arch contributes to the formation of a short yet distinct transverse process that supported the cervical rib (not preserved). The neurocentral suture is fused. The prezygapophysis is damaged (incomplete), but the postzygapophysis is distinct and bears a well-developed epipophysis dorsally. Between the pre- and postzygapophyses the neural arch shows a slight elevation with a weakly convex dorsal margin, which is all there is in terms of a rudimentary neural spine, or rather neural crest. Thus, *Dinocephalosaurus orientalis* lacks the anterodorsal expansion of the axial neural spine seen in tanystropheids (Spiekman *et al*. 2021).

Behind the axis, the third through to the 18th cervical vertebrae are preserved in an undisturbed, articulated string of vertebrae that is bent backwards. The morphology of the cervical vertebrae is generally very similar throughout this section of the neck (Fig. 6b, c). The vertebrae are distinctly elongated, increasing in length all the way up to the 18th cervical vertebra, the last one preserved in articulation. The ventral margin of the centrum is distinctly concave in lateral view, similar to that seen in *Augustaburiania vatagini* (Sennikov 2011). The articular facets for the cervical ribs are located closely together, low on the centrum near its anterior margin. The neurocentral suture is obliterated. The postzygapophysis is slender and underlain by the more massively built prezygapophysis, the latter terminating in a deep, rounded (anteriorly convex) tip. Dorsal to the postzygapophysis, a pronounced, slender and lateromedially narrow epipophysis is present, which extends posteriorly beyond the articular facet of

https://doi.org/10.1017/S175569102400001X

Table 1 Length and height of the cervical vertebrae, specimens ZMNH M8727, IVPP V13898, IVPP V0666, and ZMNH M8752. Abbreviation: CV = cervical vertebra. The length was measured across the ventral margin of the centrum; the height was measured across mid-centrum and includes the neural crest. All measurements are in mm. The measurements of ZMNH M8752 are approximate only, which is due to the tight articulation between vertebrae, as well as to the cervical ribs often obscuring the ventral margin of the centrum. Superscripts: 1 = estimate; 2 = incomplete element; 3 = element is missing part of the centrum, but the ventral limit of the bone can be accurately measured from the impression of the bone in the matrix; 4 = includes a fine crack running through the element; 5 = element partially crushed and distorted; 6 = element minimally obscured along the margin; 7 = unclear where the articulation between the centra lies. Combined length of centra 25 + 26 is 189.

	ZMNH M8727		IVPP V13898		IVPP V0666		ZMNH M8752	
Element	Length	Height	Length	Height	Length	Height	Length	Height
Atlas	–	–	–	–	12.0[1]	–	–	–
Axis	24	21.8	21	20	27[2]	23.5	–	–
CV 3	–	–	35	13	38.5	19.3	partially exposed	–
CV 4	51.9	14.8	46	14[3]	51.8[4]	20.3[4]	37.6	13.1
CV 5	63.9	16	53.5	13	63.5	18.4	46	12.1
CV 6	72.7	14.9	62.5	14	65.7	19	49.5[5]	9.0[5]
CV 7	78.2	17	66	14	69.9	19.5	56.5[5]	13.6
CV 8	81	17.6	65	15	70.9	21.2	–	–
CV 9	88	19.2	69	17	51.5[2]	21.2	–	16.4
CV 10	90.0[1]	20	68	17.5	–	–	76.0[4]	15.0[6]
CV 11	84.4[1]	21.9	74	19	71.0[2]	25.4	71.5	–
CV 12	87.4	23	75	18	84.2	24.7	86.0[4]	–
CV 13	93.3	21.7	78	20	86.5	26.8	65	19.7
CV 14	93.0[1]	–	85	21.5	87.8	28.6	80.0[7]	18.5
CV 15	96.5	22.3	84	21	88.4	31.6	84.0[7]	21.2
CV 16	100.5	23.9	91	19	87.2	32.8	86.0[7]	20.1
CV 17	101.2	24	94[1]	21	82.3	37	94.0[7]	18.6
CV 18	111	–	96	22	–	–	93.0[7]	20.5
CV 19	–	–	90[1]	24	–	–	93.0[7]	19.4
CV 20	–	–	80[1]	22[1]	–	–	94.0[7]	19.8
CV 21	–	–	82[1]	30	–	–	93.0[7]	21.3
CV 22	112.5	–	76	34	–	–	94.0[7]	19.9
CV 23	–	–	70	36.5	–	–	–	–
CV 24	109	–	64	38	–	–	–	–
CV 25	91.5[7]	–	55	35	–	–	–	31
CV 26	89.5[7]	–	48	35	–	–	70.0[6]	36.5
CV 27	85	–	45	38	–	–	66.5[6]	38.0[5]
CV 28	50[2]	–	42	–	–	–	–	38
CV 29	–	–	–	–	–	–	–	–
CV 30	–	–	–	–	–	–	–	–
CV 31	40.1	–	–	–	–	–	–	–
CV 32	–	–	–	–	–	–	–	–

postzygapophysis, as in the long-necked tanystropheids *Tanystropheus* spp., *Amotosaurus rotfeldensis*, *Raibliania calligarisi*, *Augustaburiania vatagini* and *Fuyuansaurus acutirostris* (Spiekman *et al*. 2021). The neural spine is represented by a low neural crest with a weakly concave dorsal margin that dorsally expands between the pre- and postzygapophysis, which is similar to the condition seen in *Amotosaurus rotfeldensis* and *Augustaburiania vatagini* (Fraser & Rieppel 2006; Sennikov 2011). The cervical neural spines do not bear mammillary processes, nor are they transversely expanded distally to form a spine table, in contrast to several archosauromorph taxa, including certain tanystropheids (Pritchard *et al*. 2015; Ezcurra 2016; Scheyer *et al*. 2020; Spiekman *et al*. 2021). Generally, this neural crest becomes progressively more distinctly developed in an antero-posterior gradation within this articulated series of cervical vertebrae.

Behind the series of 18 articulated cervical vertebrae a set of six partially or fully disarticulated cervical vertebrae is located, which retain the distinctly elongated morphology. Of these, four elements continue the string of the 18 articulated elements across an area damaged by breakage. Two elements are fully disarticulated and oriented at an angle relative to the long axis of the articulated cervical column. Within this set of six cervical vertebrae, an increasingly more prominent development of the neural crest is the only distinctive feature that distinguishes them from more anterior cervical vertebrae. The neural crest is most prominently developed in a vertebra that is fully disarticulated and dislocated, lying somewhat to the side with its postzygapophysis pointing in an anterior direction relative to the whole skeleton. By virtue of its well-developed neural crest, this element is identified as the 24th cervical (Fig. 6c). The 25th to the 28th cervical vertebrae again form an articulated series, preserved in reverse orientation relative to the anterior series of the 18 articulated cervical vertebrae. The 28th cervical is incompletely preserved, whereas the neural crest on the 27th cervical is either incompletely preserved or incompletely exposed. The 25th and 26th cervical vertebrae document a further elaboration of the neural crest, which gains in height particularly in its posterior part, and acquires a more pronounced convex dorsal margin.

With reference to other specimens of *Dinocephalosaurus orientalis* to be described below, more posterior cervical vertebrae are known to be much shorter in length compared to the preceding cervical vertebrae and to approach the morphology of anterior dorsal elements. A string of nine shortened but otherwise incompletely exposed posterior cervical vertebrae and/or anterior dorsal vertebrae lies in front of the preserved elements of the pectoral girdle. On the basis of associated relatively short posterior cervical ribs, four out of the string of nine vertebrae in front of the elements of the pectoral girdle are identified as shortened posterior cervical vertebrae. The next element in the series is overlain by a dorsal rib, which might have been associated with it. It is therefore counted as one out of five anterior dorsal

https://doi.org/10.1017/S175569102400001X

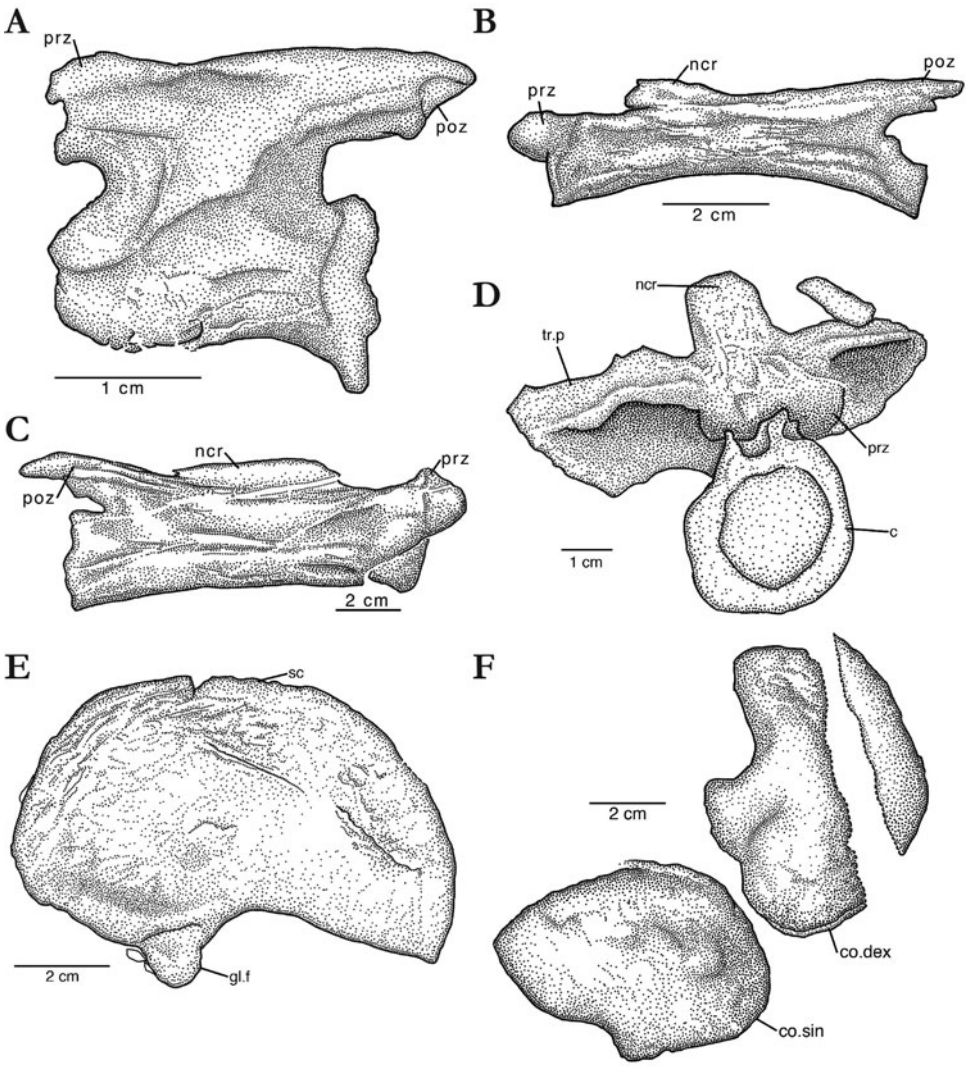

Figure 6 *Dinocephalosaurus orientalis*, ZMNH M8727, interpretative drawings of selected postcranial elements. (a) Axis in left lateral view. (b) Sixth cervical vertebra in left lateral view. (c) Posterior cervical vertebra (between 18th and 24th) in right lateral view. (d) Anterior dorsal vertebra in anterior view. (e) Right scapula in medial view. (f) Both coracoids, right coracoid in medial view and left coracoid in lateral view. Abbreviations: c = centrum; co.dex = right coracoid; co.sin = left coracoid; gl.f = glenoid facet; ncr = neural crest; poz = postzygapophysis; prz = prezygapophysis; sc = scapula blade; tr.p = transverse process.

vertebrae preserved in the series. Including the atlas and the axis, the vertebral count for the cervical region is thus a string of 18 fully articulated elements that includes the atlas and axis, two dislocated elongated elements, another section of four articulated elongated elements of which the last one is the 28th cervical, and a minimum of four shortened, posteriormost cervical vertebrae, which amounts to a total of 32 cervical vertebrae.

The cervical ribs are typical of non-crocopodan archosauromorphs, much elongated and aligned parallel to the ventrolateral margin of the cervical series of vertebrae. A distinct, free-ending anterior process projects beyond the articular head of the rib. The latter is oriented at a right angle to the shaft of the rib and articulates on a facet located low on the centrum near the latter's anterior margin. As preserved, the cervical ribs are deflected away from the posteriorly bent neck (Fig. 4). In their natural orientation, ribs associated with the fourth cervical vertebra would have bridged three successive intervertebral joints; the rib associated with the eighth cervical would have bridged five successive intervertebral joints; the rib associated with the 13th cervical would also have bridged five succeeding intervertebral joints. Cervical ribs extend the length of two or more cervical vertebrae in *Protorosaurus speneri*, *Pectodens zhenyuensis* and most tanystropheids, except for *Tanytrachelos ahynis* and *Langobardisaurus pandolfii*, which have relatively shorter cervical ribs (Spiekman *et al*. 2021). In the posterior part of the cervical vertebral column, where the vertebrae become shorter, the cervical ribs likewise become shorter, and at the same time more massively built, as is also the case in tanystropheids.

Partially overlapping the laterodorsal aspect of the (articulated) 18th cervical is a disarticulated anterior dorsal vertebra that is beautifully exposed in anterior view (Fig. 6d). The entire height of the element, from the ventral margin of the centrum to the tip of the neural spine, is 73.1 mm; the total width across the transverse processes is 85 mm. The height of the centrum alone is 34.7 mm and its width is 33.9 mm. The articular surface of the centrum is of rounded circumference, amphicoelous, and the centrum is non-notochordal. The neural canal is of rectangular contours, the massive prezygapophyses projecting from its dorsal margin. A distinct neural spine, which is not transversely expanded distally, rises up from the neural arch behind the prezygapophyses. Laterally, the neural arch is developed into deep transverse processes. Their tall distal articular surface faces ventrolaterally. In *Dinocephalosaurus orientalis*, the transverse processes of the posteriormost cervical vertebrae and anterior dorsal vertebrae are very distinctively differentiated in that their anterior surface is deeply excavated (concave) and their

https://doi.org/10.1017/S175569102400001X

posterior surface correspondingly convex in lateral view (see below). The dorsal surface is flat, the anterodorsal margin forming an overhanging shelf. A second anterior dorsal is incompletely exposed in the area between the 18th and 27th cervical.

A number of disarticulated dorsal ribs are preserved, scattered across the specimen (Fig. 4). They are evenly curved and show a slight distal expansion. Their proximal articular head is distinctly expanded to match the articular surface on the tall transverse process of the dorsal vertebrae. In addition to the cervical and dorsal ribs, scattered gastral ribs are likewise preserved. Generally slender and of delicate structure, they display two different morphologies. The medioventrally located elements are slightly angulated and taper to a fine tip on both sides. The collateral elements are weakly but evenly curved, terminating in a blunt tip proximally and in a finely pointed tip distally. Although disarticulated, the dense accumulation of gastralia suggests they formed a tightly bundled gastral basket.

2.4.3. The pectoral girdle and forelimb. Of the elements of the pectoral girdle, both coracoids are preserved lying next to one another (Fig. 6f). They form kidney-shaped plate-like elements 77 mm long (left coracoid) and 51 mm deep (right coracoid). A well-demarcated peduncle carries the ventral part of the glenoid facet. The coracoid foramen is located below and somewhat in front of this glenoid 'process'. The right scapula is dislocated but fully exposed (Fig. 6e). Again, a kidney-shaped plate-like element 98 mm long and 63.5 mm deep, it carries a glenoid 'peduncle' or 'process' that, together with its counterpart on the coracoid, completes the glenoid facet. A kidney-shaped scapula with a semicircular scapular blade is typical of *Dinocephalosaurus orientalis*, *Pectodens zhenyuensis* and tanystropheids among archosauromorphs (Spiekman *et al*. 2021), and it is absent in other archosauromorphs, including the non-crocopodans *Protorosaurus speneri* and *Prolacerta broomi* (Gottmann-Quesada & Sander 2009; Spiekman 2018). The shape of the anterior margins of both the scapula and coracoid suggests that a scapulocoracoidal fenestra, as is present in tanystropheids, is absent in *Dinocephalosaurus orientalis*. This observation is corroborated in IVPP V20295, which preserves an articulated scapulacoracoid (see below). The left scapula is only partially exposed, but its posteroventral portion protrudes from below the left coracoid. The anterior part is developed into a broad plate, the exact contours of which remain concealed by the overlapping coracoid. Posteriorly, the element appears to extend into a robust posterior stem that tapers to a blunt tip. A broken curved ossification located near the left coracoid could represent an incomplete clavicle, but it could also be a fragment of a dorsal rib.

Both the left and the right humeri are well preserved and exposed (Fig. 4). They are slightly curved elements which, due to skeletal paedomorphosis, show little morphological differentiation. An entepicondylar foramen is absent. The ectepicondylar groove is shallow, with a weakly expressed ectepicondylar notch at its distal end. Only a fragment of the distal end of the left radius is preserved. Of the left ulna, only the distinctly expanded proximal part is exposed. The right zeugopodium is more completely preserved and exposed, although overlying ribs again obscure parts of the elements. The proximal end of the ulna is more distinctly expanded than that of the radius, whereas distally the radius is more massively built than the ulna. A total of seven rounded carpal ossifications are scattered across the slab distal to the stylopodial and zeugopodial elements, as are five, possibly six, metacarpals and a number of phalanges (Fig. 4). These autopodial elements evidently derive from both hands. Their disarticulation and incompleteness do not allow a reconstruction of the structure of the manus.

2.5. Referred specimen, ZMNH M8728

(Figure 7). The exposed parts of the skeleton comprise a partially preserved skull exposed in right lateral view; the cervical and most of the dorsal vertebral column represented by 56 vertebrae preserved in articulation (32 cervical vertebrae and 23 dorsal vertebrae), cervical and dorsal ribs; elements of both pectoral girdles and forelimbs; and the gastral rib basket. The posterior part of the dorsal column, sacrum, pelvic girdles and hindlimbs, as well as the tail, are missing (Fig. 7).

2.5.1. The skull and mandible. The incompletely preserved right side of the skull and the right mandible are preserved in articulation. The body of the right premaxilla shows five tooth positions with the first four teeth preserved *in situ* and the fifth tooth being broken. The third premaxillary tooth is the largest, given that the fourth tooth position shows an erupting replacement tooth. The tooth crown is recurved and pointed, covered by striated enamel towards the apex. Behind the premaxilla extends a strip of bone that represents the partially preserved and exposed maxilla; the maxillary tooth row is not preserved or exposed, except for two alveolar sockets located at the level of the anterior margin of the orbit. A gap located behind the body of the premaxilla, separating the preserved/exposed part of the maxilla from a sheet of bone that represents the nasal, most probably corresponds to the antorbital recess. Posterior to the maxilla and nasal lies a well-defined, vertically oriented, semi-lunar prefrontal with a strongly convex anterior margin, and a concave posterior margin that defines the anterior margin of the orbit, which is typical of early archosauromorphs, including tanystropheids (e.g., Flynn *et al*. 2010; Miedema *et al*. 2020; Spiekman *et al*. 2020b). Crushed and distorted parts of the parietal skull table, involving the frontal and parietal, are exposed at the dorsal margin of the skull above the orbital and temporal region. Crushed bone fragments, which are posterodorsally located and offer no anatomical detail, most probably represent remains of the braincase. The right pterygoid is very well preserved (Fig. 8b) and exposed below the posterior part of the maxilla, the orbit and the temporal region. The palatine ramus of the pterygoid can be seen reaching far forward to a level well in front of the prefrontal, although its further anterior extent disappears below the remains of the maxilla. The prominent and rounded transverse process is deflected ventrally as a consequence of distortion, and exhibits a strongly rugose lateral surface, which is similar to that seen in *Tanystropheus hydroides* (Spiekman *et al*. 2020b). The quadrate process of the pterygoid is revealed to be rather deep in lateral view. It terminates in a tall posterior edge that has separated from the crushed quadrate lying behind it. Within the area of the orbit, behind the posterior end of the exposed part of the maxilla and located right at the base of the palatine ramus of the pterygoid, lie a couple of trapezoid-shaped ossifications, their lateral margins slightly convex. Given their intact preservation and location, these elements are identified as ectopterygoids.

The right mandibular ramus is preserved in right lateral view (Fig. 8a); from below it emerges the lower margin of the left mandibular ramus, with the left dentary sheared off and exposed ventrally. The anterior tip of the dentary is slightly broadened to form a fortified mandibular symphysis. The largest dentary teeth, four in number, follow two or three much smaller anterior dentary teeth. The four enlarged dentary teeth would thus come to lie in between the premaxillary and the maxillary fangs. The dentary tooth row is not completely preserved, but with 14 complete and incomplete dentary teeth preserved *in situ*, a total of 19–21 tooth positions can be assumed. While the enlarged anterior dentary teeth are still somewhat recurved, those located behind them are straight upright. Again, the dentary teeth are pointed, their enamel covering striated towards the apex of the crown. Some of the more posteriorly located dentary teeth show plicidentine infolding at their base. If any coronoid process were developed it could form a weak elevation only, obscured by the overlapping transverse process of the pterygoid. A

https://doi.org/10.1017/S175569102400001X

Figure 7 *Dinocephalosaurus orientalis*, ZMNH M8728 (referred specimen). (a) Photograph. (b) Interpretative drawing. Abbreviations: cl = clavicle; co = coracoid; co-sc = articulated coracoid and scapula; cr = cervical rib; cv = cervical vertebra; hu = humerus; ns = neural spine; ra = radius; ul = ulna.

retroarticular process is again confirmed to be reduced in size. Sutural details are hardly identifiable except for the partial posterior delimitation of the dentary. What looks like a sinuously curved crack in the postdentary part of the mandible might represent the natural separation of the dorsally located surangular from the ventrally located angular.

2.5.2. The vertebral column. (Table 2). The atlas is not identifiable and the axis is only partially exposed, crushed between the posterior end of the right mandibular ramus and bone fragments that most probably represent remnants of the braincase. But from the third cervical vertebra on backwards, the entire cervical and most of the dorsal region is beautifully preserved in articulation (with a break between cervical 23 and cervical 24), and exposed in right lateral view (Fig. 7). Cervical vertebrae 3 through to 28 show the elongated morphology also characteristic of the other specimens of *Dinocephalosaurus orientalis.* The length of the centrum increases steadily from cervical vertebra 3 to cervical vertebra 23, behind which it decreases again more rapidly. Up to cervical vertebra 24, the ventral margin of the centrum is strongly concave in lateral view, which gives the impression of a markedly expanded anterior and posterior intervertebral articular facet. The articular facets for the cervical ribs

https://doi.org/10.1017/S175569102400001X

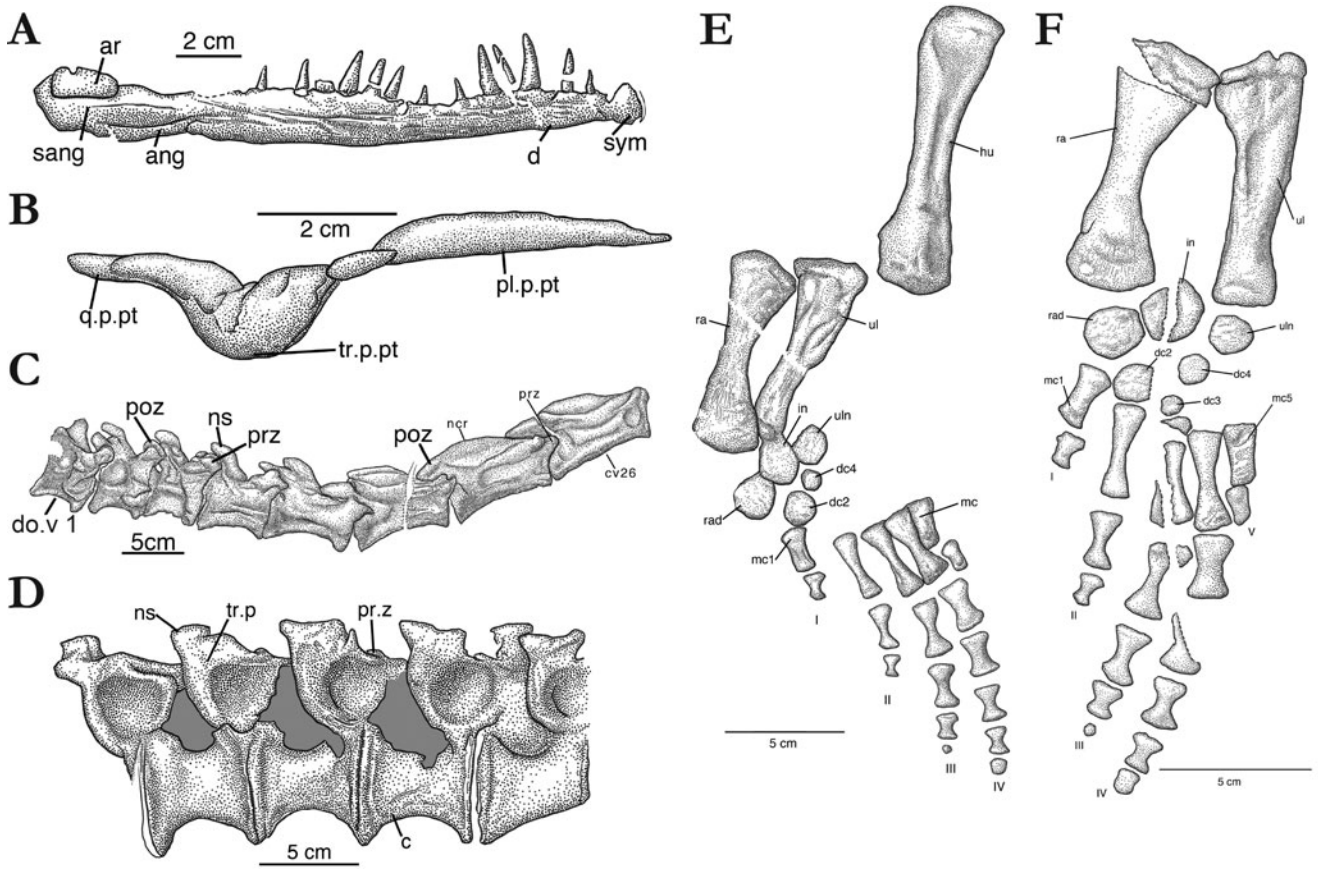

Figure 8 *Dinocephalosaurus orientalis*, ZMNH M8728, interpretative drawings of selected elements. (a) Right mandibular ramus in lateral view. (b) Right pterygoid in lateral view. (c) Posterior cervical vertebrae and anteriormost dorsal vertebra (cv26–do.v1) in right lateral view. (d) Mid-dorsal vertebrae in right lateral view. (e) Right forelimb, as preserved. (f) Left forelimb, as preserved. Abbreviations: ang = angular; ar = articular; c = centrum; cv = cervical vertebra; d = dentary; dc = distal carpal; do.v = dorsal vertebra; hu = humerus; int = intermedium; mc = metacarpal; ncr = neural crest; ns = neural spine; pl.p.pt = palatine process of the pterygoid; poz = postzygapophysis; prz = prezygapophysis; q.p.pt = quadrate process of the pterygoid; sang = surangular; sym = symphysis; tr.p = transverse process; tr.p.pt = transverse process of the pterygoid; ra = radius; rad = radiale; ul = ulna; uln = ulnare.

lie low on the centrum near its anterior margin. The prezygapophysis is again shorter and more massively built than the postzygapophyses, the latter bearing prominent epipophyses that extend beyond the posterior margin of the centrum as it tapers to a pointed tip. Up to cervical vertebra 24, the neural crest is extremely shallow, its concave dorsal margin resulting in weakly expressed anterior and posterior dorsal projections located between the pre- and postzygapophyses respectively. The neurocentral suture is fused; there is no indication that the vertebral centra would be hollow, as they are in *Tanystropheus* (Wild 1973; Spiekman *et al*. 2020b).

A transition in the morphology of the cervical vertebrae starts with cervical 26 (Fig. 8c). Somewhat shorter already (see Table 5), the vertebra gains in depth, the ventral margin of the centrum being less concave in lateral view, the neural crest more prominently developed and with a straight dorsal margin. Posteriorly, the neural crest develops into a posterior projection that overhangs the zygapophyseal articulation. Pre- and postzygapophyses are more symmetrically developed, projecting less beyond the anterior and posterior margins of the centrum than in more anteriorly located cervical vertebrae. In cervical vertebra 27, the same trend of morphological transformation continues, culminating in cervical vertebra 28, which again has diminished in length compared to the directly preceding vertebrae. The central margin of the centrum is only slightly concave in lateral view; the neural crest is rather prominently developed with a distinctly convexdorsal margin, and it carries a posterior projection that extends well beyond the zygapophyseal articulation. In addition, the diapophysis, which in preceding cervical vertebrae was positioned directly adjacent to the parapophysis near the anteroventral end of the centrum, has shifted dorsally onto about the mid-height of the centrum.

Further modifications occur in more posterior cervical vertebrae as these lead up to the anterior dorsal vertebrae (Fig. 8c). The length of the centrum decreases rapidly, whereas its depth increases, such that the centrum of cervical vertebra 32 has acquired the proportions characteristic of dorsal vertebrae. The ventral margin of the centrum becomes more pronouncedly concave again in lateral view. The articular facets for the cervical rib are increased (to match the size of the articular heads of the short and more massively built cervical rib), with the diapophysis being positioned further dorsally, possibly being placed partially on the neural arch, and a laterally projecting crest develops that runs from the diapophysis backwards along the length of the centrum. Pre-and postzygapophyses are symmetrically developed, and between them rises up a prominent yet slender, curved, finger-like neural spine pointing posterodorsally, which is a morphology that is apparently unique among early archosauromorphs. The 32rd presacral vertebra can be identified as a cervical based on its position distinctly anterior to the pectoral and its short associated rib that is oriented mostly posterior and slightly ventral to the vertebral column (i.e., a rib that therefore does not contribute to the rib cage of the trunk). The 36th presacral vertebra can be identified as a dorsal element, as it is associated with a dorsal rib (i.e., a rib that curves ventrolaterally from its head to contribute to the rib cage). The 33rd presacral vertebra has only a partial rib associated with it, whereas no ribs are preserved in association with the 34th and 35th presacral vertebrae, and these elements might be considered transitional elements.

https://doi.org/10.1017/S175569102400001X

Table 2 Length and height of the presacral vertebrae, specimens IVPP V20295 and ZMNH M8728. Abbreviations: CV = cervical vertebra; PSV = presacral vertebra. The length was measured across the ventral margin of the centrum; the height was measured across mid-centrum and includes the neural crest. All measurements are in mm. Superscripts: 1 = not completely exposed; 2 = dorsals 5 and 6 are slightly distorted; 3 = element marginally obscured; 4 = approximate length as the element is broken.

	IVPP V20295		ZMNH M8728			IVPP V20295		ZMNH M8728	
Element	Length	Height	Length	Height	Element	Length	Height	Length	Height
					PSV 33	–	–	37.5	61.5[3]
Atlas	–	–	–	–	PSV 34	–	–	36.8	–
Axis	23.6	23.9	24.1[1]	16.5	PSV 35	–	–	–	–
CV 3	40	19.3	38.9	17.5	PSV 36	33.4	–	35.5	55.9
CV 4	54.4	19.8	50.5	17.8	PSV 37	34.7	–	32	54.8
CV 5	–	20.3	59.5	17.6	PSV 38	29.0[2]	57.9	–	–
CV 6	–	20.5	69.4	17.9	PSV 39	28.5[2]	60.2	–	–
CV 7	69.8	20.1	79.2	18.7	PSV 40	–	–	34.4	51.5[3]
CV 8	69.6	21.7	78.5	18.3	PSV 41	–	–	31.9	62.7
CV 9	73.3	20.7	82.1	18	PSV 42	33.4	64.8	32.6	61.2
CV 10	74.7	23.6	84.5	21.5	PSV 43	–	–	32	60
CV 11	74.5	25	86	22	PSV 44	–	–	34.7	61.1
CV 12	76.5	24	82.0[4]	24.6	PSV 45	–	–	31.7	62.3
CV 13	77.4	25	–	25	PSV 46	–	–	–	64.3
CV 14	77.3	25	89.5[4]	25.2	PSV 47	41.2	–	–	63
CV 15	84.1	–	90.6	26.9	PSV 48	–	–	33.2	62
CV 16	84.6	25.2	92.1	25.2	PSV 49	–	–	31.6	62.3
CV 17	88.5	26.1	98.3	26.7	PSV 50	33.6	–	31.3	64.1
CV 18	89.9	25.4	100.2[1]	26.4	PSV 51	29.3	–	30.8	63.4
CV 19	90.2	26.2	97.2	26.2	PSV 52	–	–	30.9	60.6
CV 20	89	28.3	100.6	27.4	PSV 53	31.3	63.9	29.2[3]	55.2
CV 21	–	31.7	110.7	28.2	PSV 54	31.4	64.8	–	–
CV 22	–	38.7	105.5[3]	29.5	PSV 55	–	–	–	–
CV 23	–	–	115.8[1]	32.5	PSV 56	–	–	–	–
CV 24	–	–	105.7	28.1	PSV 57	–	–	–	–
CV 25	–	–	99.8	43.8	PSV 58	33.1	–	–	–
CV 26	67.4	43	92.3	48.8	PSV 59	29.8	–	–	–
CV 27	57.3	49.5	82.9	48.4	PSV 60	30.9	–	–	–
CV 28	45.6	54.2	73.5[1]	49.5	PSV 61	30.6	–	–	–
CV 29	–	54.4	63.8	55.4	PSV 62	30.6	–	–	–
CV 30	–	–	50.5	60.9					
CV 31	–	–	37.6	60.2					
CV 32	–	–	38.5	60.6					

The anterior cervical ribs are much elongated, their shaft aligned along the long axis of the cervical vertebral column (Fig. 7). The rectangular articular heads, which are set parallel to each other, are oriented at a right angle relative to the long axis of the shaft, and the cervical rib terminates anteriorly in an elongate free-ending, anterior process. The ribs associated with cervical vertebrae 3 and 4 are clearly identifiable, which leaves the shafts of a total of four cervical ribs bridging the intervertebral joint between axis and cervical 3. This confirms that the first pair of cervical ribs articulated on the atlas. It is noteworthy that the shaft of these anteriormost cervical ribs is much elongated already, as its posterior tip lies behind the intervertebral joint between cervical 3 and 4. Towards the middle and more posterior parts of the neck, cervical ribs may bridge up to five or six intervertebral joints. The last of these slender, much elongated cervical ribs, articulating with cervical vertebra 27 and – possibly – cervical vertebra 28, terminate posteriorly just in front of, or below, cervical vertebra 32 and the first dorsal vertebra. Starting with cervical vertebra 29, the cervical ribs undergo a characteristic modification, which also occurs in other long-necked archosauromorphs like *Tanystropheus* spp. and *Tanytrachelos ahynis* (Olsen 1979; Rieppel *et al*. 2010): they become much more robustly built and shorter. The articular head increases in relative size, as does the free-ending anterior process, while the posteriorly extending shaft is short, distinctly curved, and terminating in a pointed tip.

A string of 21 dorsal vertebrae is preserved, the last one in the series only incompletely so. The centra of the dorsal vertebrae are both laterally and ventrally strongly constricted (Fig. 8d). The neural arch of the dorsal vertebrae is very robust, being in that regard more similar to that seen in sauropterygians than that of archosauromorphs (Rieppel 2000; Ezcurra 2016; Spiekman *et al*. 2021). Pre- and postzygapophyses are symmetrically differentiated and do not project far beyond the anterior and posterior margins of the centrum. The well-developed transverse processes are of a rather peculiar morphology: they are very tall in their dorso-ventral dimension, but slender in their antero-posterior dimension. Their anterior surface is deeply excavated or concave, which translates into a prominently convex posterior surface. As was described above, cervical vertebrae 29 through to 32 develop a prominent neural spine that forms a slender, posterodorsally curving projection. With presacral vertebra 33 begins a reduction in the relative size of the neural spine that continues through to the 40th and 41st presacral vertebra. Further posteriorly, the development of the neural spine becomes more prominent again, now assuming rectangular contours in lateral view. Their anterior and posterior margin is slightly concave in lateral view, whereas their dorsal margin is either straight or slightly convex. The dorsal ribs are evenly curved and show a slight distal expansion. Their proximal articular head is much expanded into a triangular structure that matches the height of the transverse processes.

https://doi.org/10.1017/S175569102400001X

The gastral rib basket is well preserved, albeit mostly disarticulated (Fig. 7). Some of the gastral ribs retain their natural configuration, however, showing that each gastral rib is composed of three elements, an angulated medioventral one, the apex pointing forwards, and one collateral element on either side, forming an overlapping contact. The collateral elements are slender, pointed at both ends, and weakly curved dorsally in their lateral part. The gastral basket was clearly tightly bunched.

2.5.3. The pectoral girdle and forelimb. Despite the pectoral girdle of ZMNH M8728 being otherwise complete and the entire skeleton being largely in articulation, an interclavicle is not preserved, nor is it in any other known specimen of *Dinocephalosaurus orientalis*. This suggests that an ossified interclavicle was probably absent in this taxon, as is also the case in *Tanystropheus* spp. and *Ozimek volans* (Spiekman *et al*. 2021). The right clavicle is broken across the transition from the cervical to the dorsal vertebral column. The anterior (medial) part of the left clavicle protrudes from below the right scapula (Fig. 7). The clavicle is an evenly curved, blade-like element, with its anterior (medial) end slightly set off by a weak constriction. The right scapulocoracoid is well preserved and exposed in articulation; it overlaps, and thus partly obscures, the left scapulocoracoid. The right coracoid forms a kidney-shaped element with the dorsal 'glenoid process' located in its posterodorsal part. The coracoid foramen is located just anteroventral to this 'glenoid process', and it is fully enclosed by bone. The length of the coracoid is 93 mm and its depth is 47 mm. The scapula again forms a kidney-shaped element with a 'glenoid process' located at its anterior end, which together with its counterpart from the coracoid completes the glenoid facet. The length of the right scapula is about 82 mm and its depth is 67.8 mm.

The right humerus is well preserved and exposed (Figs 7, 8e); the distal end of the left humerus protrudes from below the two coracoids and passes below the distal end of the right humerus. In ZMNH M8728, the (right) humerus is a rather straight element, unlike in ZMNH M8727, where it appears curved. Possibly, this is the result of the angle under which the elements are exposed, which cannot be discerned confidently due to the lack of observable features (attributable to paedomorphosis). Its proximal and distal ends are expanded, which results in a biconcave shaft. Little morphological detail is differentiated or identifiable. An entepicondylar foramen is absent. The ectepicondylar groove and (distal) notch are weakly expressed. Both the right and the left zeugopodium are well preserved and exposed (Fig. 8e, f). The radius and ulna are subequal in length, the ulna being just a bit shorter than the radius (see Table 3). The radius is a bit more robustly built than the ulna. It is expanded proximally as well as distally to a similar degree, which results in a biconcave shaft. The concavity of the postaxial margin of the shaft, defining the spatium interosseum, is more pronounced than the concavity of the preaxial margin of the shaft. The ulna is markedly expanded proximally but only weakly expanded distally. An ossified olecranon is absent. The preaxial margin, defining the spatium interosseum, is concave; its preaxial margin is rather straight instead, with a weak concavity expressed at the distal end.

Five carpal ossifications are preserved in the right manus (Fig. 8e) and six in the left autopodium (Fig. 8f). In both hands, there are three proximal carpal ossifications, and two versus three distal carpal ossifications, respectively. In the right manus, the irregularly polygonically shaped proximal carpals are preserved in articulation (sutural contact) and comprise the radiale (maximum exposed length: left, 19.2 mm; right, 19.6 mm), intermedium (left, 21 mm; right, 20.7 mm) and ulnare (left, 13,6 mm; right, 15.2 mm). Of those, the intermedium is the largest and the ulnare the smallest. In the distal carpal row of the right hand, a distinctly larger element lies in a preaxial position relative to the smaller distal carpal located postaxially. The same two distal carpals of similar relative size can be identified in the left manus, where the larger preaxially located element lies proximal to metacarpal II. The somewhat smaller postaxially located element is situated proximal to metacarpal IV, albeit a bit removed from it. A much smaller third distal carpal is located in between the two aforementioned elements, situated proximal to metacarpal III. This latter element has been lost or failed to ossify in the right manus. In ZMNH M8728, there are thus three distal carpals ossified, of which dcII is the largest, dcIII the smallest, and dcIV is intermediate in size.

Of the five metacarpals (Fig. 8e, f), the first through to the fourth are relatively elongated, slender elements with a biconcave shaft. Amongst them, the third and the fourth are the longest. The fifth metacarpal is distinctly shorter, approximately of the same length as the first metacarpal, but more sturdily built. The phalangeal count is 1–2–4–5–1 in both hands and only the digits III and IV terminate in an element that is clearly identifiable as an ungual. It thus appears that the more distal phalanges in digits I, II and V were absent or did not ossify. There is no indication of a juvenile status of this specimen, since it is of respectable adult size, and this limited phalangeal count probably represents a paedomorphism related to aquatic adaptation.

Table 3 Length and width of the individual forelimb elements in the four specimens preserving the forelimbs, ZMNH M8727, ZMNH M8728, ZMNH M8752 and IVPP V20295. Abbreviations: L = length; PW = proximal width; MW = minimal width; DW = distal width. All measurements are in mm.

		ZMNH M8727	ZMNH M8728	ZMNH M8752	IVPP V20295
Right humerus	L	121.4	127.5	–	125.0
	PW	27.5	33.5	–	29.8
	MW	23.6	~19.0	–	21.6
	DW	30.0	29.0	–	30.9
Left humerus	L	124.5	83.5	–	–
	PW	25.2	31.5	–	–
	MW	21.2	–	–	21.3
	DW	26.1	30.0	–	28.5
Right ulna	L	–	–	–	89.5
	PW	–	–	–	26.4
	MW	–	–	–	4.6
	DW	–	–	–	18.2
Left ulna	L	–	82.0	71.0	–
	PW	–	28.5	27.5	–
	MW	–	–	–	–
	DW	–	30.0	17.8	–
Right radius	L		–	–	83.3
	PW		–	–	30.2
	MW		–	–	12.4
	DW		–	–	26.5
Left radius	L	–	–	73.0	87.2
	PW	–	–	28.8	28.5
	MW	–	–	10.6	12.5
	DW	–	–	27.5	25.3
Left metacarpal I	L	–	21.0	17.5	26.0
Right metacarpal I	L	–	20.6	~20.0	25.4
Left metacarpal II	L	–	31.2	27.8	34.8
Right metacarpal II	L	–	30.8	26.7	–
Left metacarpal III	L	–	33.6	32.3	35.8
Right metacarpal III	L	–	35.0	~28.6	–
Left metacarpal IV	L	–	33.0	30.4	–
Right metacarpal IV	L	–	34.4	29.8	36.8
Left metacarpal V	L	–	20.0	–	25.1
Right metacarpal V	L	–	22.0	18.4	24.0

2.6. Referred specimen, ZMNH M8752

(Figure 9). This is one of the more complete specimens of *Dinocephalosaurus orientalis* available for study. It comprises the skull

https://doi.org/10.1017/S175569102400001X

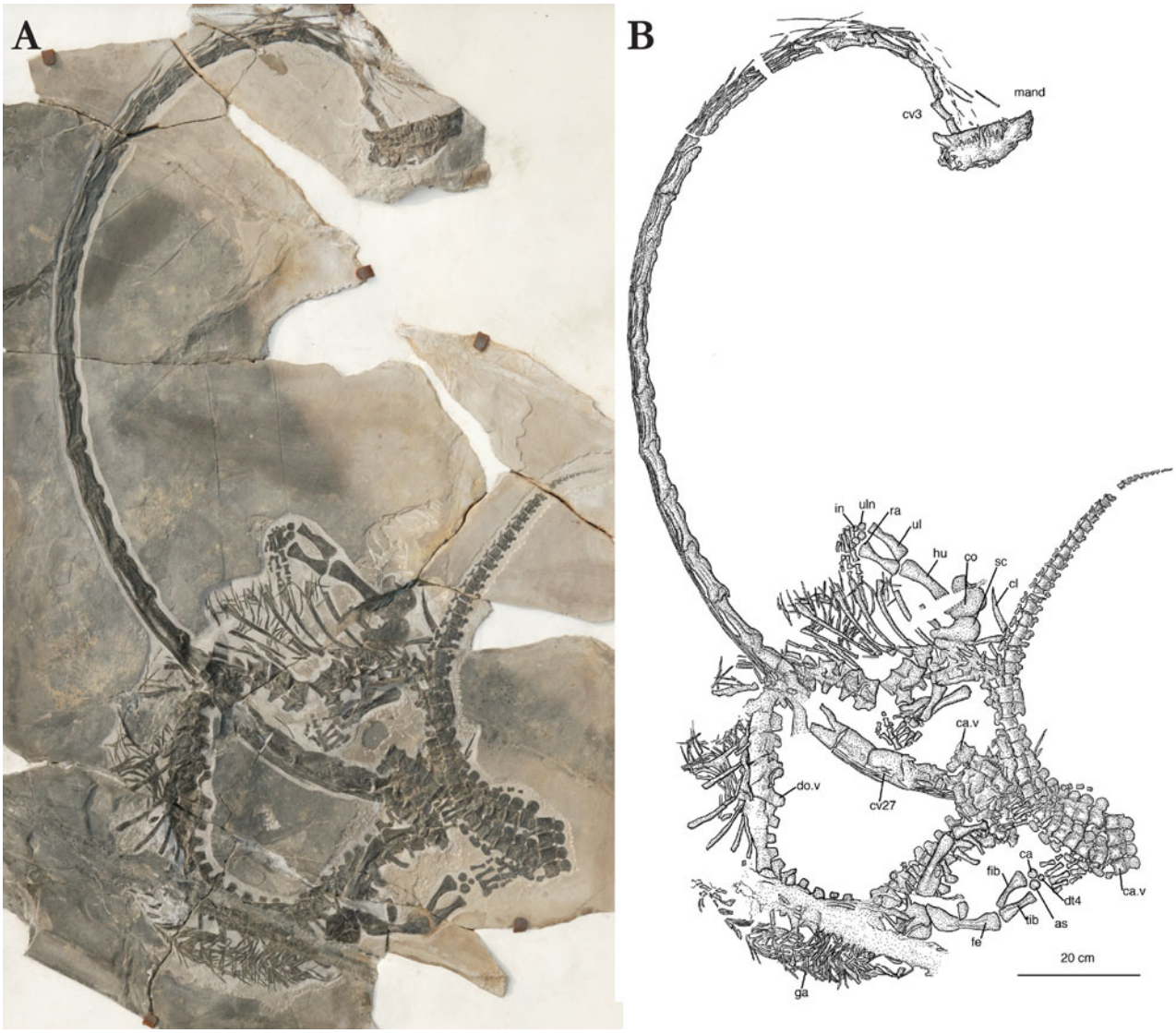

Figure 9 *Dinocephalosaurus orientalis*, ZMNH M8752 (referred specimen). (a) Photograph. (b) Interpretative drawing. Abbreviations: as = astragalum; ca = calcaneum; ca.v = caudal vertebra; cl = clavicle; co = coracoid; cv = cervical vertebra; do.v = dorsal vertebra; dt = distal tarsal; fe = femur; fib = fibula; ga = gastralia; hu = humerus; in = intermedium; mand = mandible; ra = radius; sc = scapula; tib = tibia; ul = ulna; uln = ulnare.

and mandible, neck, trunk and complete tail, ribs, gastral ribs, pectoral girdle and forelimbs as well as pelvic girdle and hindlimbs (Fig. 9). Measurements allow the assessment of the relative body proportions of this specimen, which are: skull, 16 cm; neck, 234 cm; trunk (including the sacrum), 100 cm; tail, 160 cm; total length, 510 cm. The neck is thus shown to be more than twice as long as the trunk and the tail more than 1.5 times as long as the trunk.

2.6.1. The skull and mandible. The skull and mandible are preserved in articulation and exposed in left lateral view. Preservation is such, however, that little anatomical detail is discernible. The tip of the snout is deflected to the left so as to expose the premaxillae in anterior view. As a consequence, a left and a right premaxillary fang embrace the tip of the left mandible. On the dorsal surface of the rostrum, the anterior end of the antorbital recess is particularly well exposed on the left side, lined medially by the very elongate posterior (nasal) process of the premaxilla. The remainder of the skull is preserved as a crushed mass of bone, with the isolated left squamosal rotated and exposed anterodorsal to the well-preserved and well-delineated left quadrate. The latter shows a broad expansion of the cephalic condyle atop a relatively slender shaft. The quadrate is only weakly concave posteriorly. Little morphological detail is again discernible on the mandible. As in other specimens of *Dinocephalosaurus orientalis*, the dentary is somewhat expanded anteriorly as it participates in the formation of a reinforced mandibular symphysis. There is no indication of a coronoid process. The way the specimen is preserved suggests the presence of a large, posteroventrally deflected retroarticular process, but since such is absent in other specimens of *Dinocephalosaurus orientalis*, this appearance must be due to breakage and deformation, and a dislocation of the left mandible and left quadrate relative to one another.

Three teeth are preserved *in situ* on the left premaxilla, of which the anterior two form premaxillary fangs. A total of 15 teeth are preserved *in situ* on the left maxilla, of which the anterior four are distinctly larger than the succeeding maxillary teeth. The largest maxillary fang is the fourth tooth preserved in the tooth row, behind which the maxillary teeth gradually decrease in size. A total of at least 12 dentary teeth can be counted as preserved *in situ*, of which three enlarged anterior fangs are located in between the posteriormost preserved premaxillary tooth and the anteriormost preserved maxillary tooth. This again suggests a diastema in the upper tooth row in the area of the relatively slender anterior process of the maxilla that lines the lateral margin of the anterior end of the antorbital recess housing the

https://doi.org/10.1017/S175569102400001X

external naris. It appears possible, however, that a much smaller maxillary tooth located in front of the anterior maxillary fangs is largely concealed by the third dentary fang. The large anterior fang-like teeth are only weakly recurved if at all, and the more posterior teeth are upright. All teeth are pointed, the enamel surface striated apically. Especially in the larger teeth, plicidentine infolding is apparent at the base of the tooth.

2.6.2. The vertebral column. (Table 1). The atlas and axis are not exposed in ZMNH M8752. The elongated and slender third cervical vertebra protrudes from below the left mandible. Starting with cervical vertebra 3, the cervical vertebral column is well preserved and exposed in left lateral view in an articulated series up to cervical vertebra 28 (Fig. 9). The general morphology of the cervical vertebrae is again very similar to that observed in other specimens of *Dinocephalosaurus orientalis*. The cervical vertebrae 23 through to 25 are broken and incompletely preserved, but the neck vertebrae in front of that break are longer and more delicately built than vertebrae 26 to 28. The first 20 cervical vertebrae are elongated and slender, with a very shallow neural crest that retains a concave dorsal margin in lateral view. This results in antero- and posterodorsal neural crest projections located in between the pre- and postzygapophyses respectively. The epipophyses dorsal to the postzygapophyses form a distinct, slender, posterior projection capping the more sturdily built prezygapophyses as they extend well beyond the posterior margin of the centrum. The articular facets for the cervical ribs are located low on the centrum near its anterior margin. The intervertebral articulation between the centra is somewhat obliquely oriented, slanted in an anterodorsal–posteroventral direction. The 26th through to the 28th cervical vertebrae increase in depth but decrease in length. The centrum gains in height, as does the neural crest, which develops a convex dorsal margin. In cervical 27, and even more so in cervical 28, the neural crest furthermore develops into an increasingly distinct posterior projection located in between the postzygapophyses. Up to the tenth cervical, the cervical ribs are deflected away from the posteriorly bent neck. They show the typical structure with a medially directed articular head that is oriented at right angles to the much-elongated shaft, and that carries a free-ending anterior process. Starting with cervical 11, the cervical ribs retain their natural position, together forming a tight bundle of bony rods that runs along the ventrolateral aspect of the cervical vertebral column, obscuring the ventral margin of the centra.

At the position of cervical 28, the cervical series partially disappears below four segments of the proximal caudal vertebral column that have snapped and separated but still remain clustered. At the transition from neck to trunk, the vertebral column turns around and becomes fully exposed again from below more distal parts of the tail (Fig. 9). The anterior region of the dorsal vertebral column is intersected by the neck (cervical 23 to 25). Subsequent, more posteriorly located dorsal vertebrae have been subjected to crushing, distortion or incomplete preservation. A complete count of 62 presacral vertebrae (including the non-exposed atlas and axis) is nonetheless possible, comprising 32 cervical vertebrae and 30 dorsal vertebrae.

Behind the elements of the pectoral girdle five dorsal vertebrae are located, which are well preserved and exposed (Fig. 9). They show the marked lateral as well as ventral constriction of the centrum, and the sturdily built neural arch that forms the tall, anteriorly deeply excavated transverse processes. The pre- and postzygapophyses are symmetrically developed, the plane of articulation between them horizontally oriented. The neural spine is distinct, marked by essentially rectangular contours but slanting slightly backwards. Progressing backward within the dorsal region, the neural spines become more prominent, increasing both their height as well as their antero-posterior dimension. The anterior dorsal ribs form evenly curved elements; more posterior dorsal ribs are mttore pronouncedly curved in the proximal 'shoulder' region. The dorsal ribs are distally slightly expanded and form a distinct articular head proximally.

As is true of the posterior dorsal vertebrae, the sacrum is poorly preserved (Fig. 9). It is possible to identify two sacral vertebrae, which however offer no relevant anatomical detail.

The tail in ZMNH M8752 is broken into several segments in its proximal part. A total of 69 caudal vertebrae are preserved (Fig. 9) but this is an incomplete count. The first few caudal vertebrae are partially obscured by overlying elements of the left hindlimb (femur and tibia). Caudal ribs are associated (not fused) with the first six caudal vertebrae. They decrease in both width and length in a posterior direction. Small, 'stubby' transverse processes can be identified on three more caudal vertebrae, but there is no evidence of caudal ribs being present beyond the ninth caudal. The neural spine morphology again shows significant changes within the caudal vertebral column (Fig. 10). Of essentially rectangular shape in the first six caudal vertebrae, they resemble those of the posterior dorsal vertebrae. Between the sixth and the ninth caudal vertebra, the neural spines begin to assume rounded contours (i.e., with a distinctly convex dorsal margin in lateral view), which become fully expressed beyond the ninth caudal vertebra resulting in a highly distinctive morphology. Very prominent anteriorly, the neural spines gradually decrease in size posteriorly, particularly past the 39th caudal vertebra. More posteriorly, beginning around the 40th to 43rd preserved caudal vertebrae, the neural spines start to form a posterodorsally directed projection. Prominent at first, and characterised by an anteroposterior expansion towards the distal end, the neural spines progressively decrease in size more posteriorly; the last, diminutive rudiment of a neural spine can be identified on the 65th preserved caudal vertebra. The chevrons similarly show a changing morphology along the caudal vertebral column (Fig. 10). Articulating in an intervertebral position, they form a broad plate-like ventral expansion of rounded contours in the anterior tail region, mirroring the neural spines in their structure (Fig. 10a). Again, in the area of the 40th through to the 43rd preserved caudal vertebrae, the chevrons are seen to gradually change their shape, forming an inverted T-bar, the stem of which articulates in an intervertebral position on the ventral edge of the centra (Fig. 10b, c). This morphology is not unique to *Dinocephalosaurus orientalis*, as a somewhat similar distal expansion of the chevrons is also present in *Trilophosaurus buettneri* (Spielmann *et al*. 2008). Again, the chevrons continue to gradually decrease in size in a posterior direction; the last diminutive chevron articulates on the 64th and 65th preserved caudal vertebrae respectively.

The gastral rib basket is preserved in a somewhat disarticulated condition in the anterior, middle and posterior trunk region (Fig. 9). Particularly in the anterior trunk, it can be ascertained that each gastral rib is composed of three elements: an angulated midventral element, the apex pointing anteriorly, and two collateral elements that meet the midventral element in an overlapping contact, and that are slightly curved in their lateral part.

2.6.3. The pectoral girdle and forelimb. The distal (dorsal) ends of both left and right clavicles are exposed, their proximal ends being buried below the caudal vertebral column. The distal part of the clavicle is evenly curved and tapers to a blunt tip. The left scapula is preserved in articulation with the left coracoid, which itself is incomplete. The scapular blade forms a kidney-shaped ossification with a convex dorsal and concave ventral margin that carries a glenoid process near its posteroventral end. The length of the scapula is 80 mm and its depth is 51.1 mm. The left coracoid is less well preserved, but shows the coracoid foramen to be located in its anterior part, in front of and below the glenoid facet. The right scapulocoracoid is not preserved or exposed.

https://doi.org/10.1017/S175569102400001X

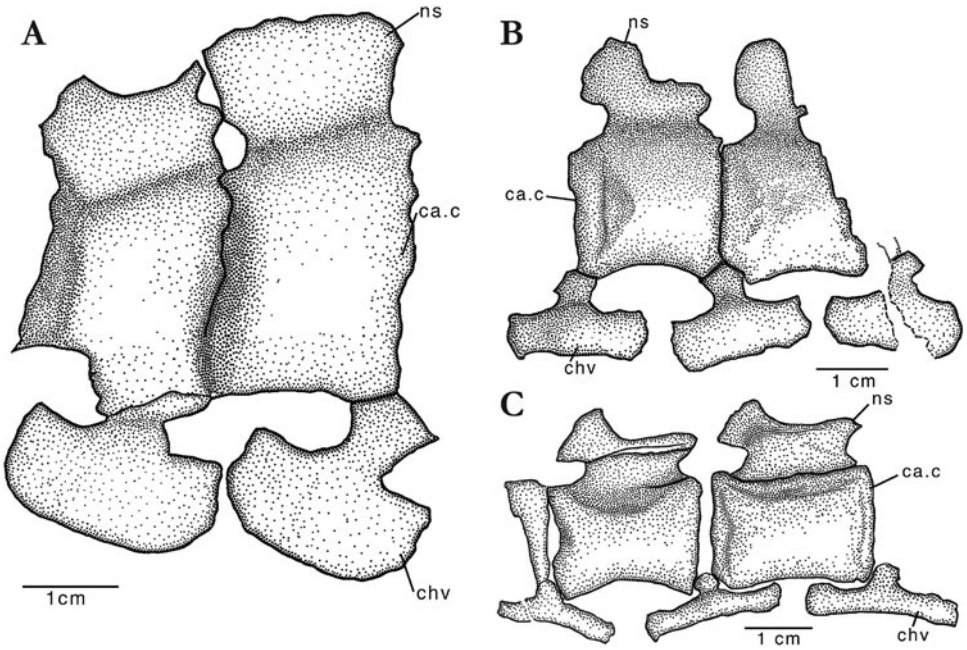

Figure 10 *Dinocephalosaurus orientalis*, ZMNH M8752, detailed drawings of selected caudal vertebrae. (a) Anterior caudal vertebraea in right lateral view. (b) Mid- to posterior caudal vertebrae in right lateral view. (c) Posterior caudal vertebrae in right lateral view. Abbreviations: ca.c = caudal centrum; chv = chevron; ns = neural spine.

Both forelimbs are preserved in ZMNH M8752, but the left one is better exposed than the right one (Table 3), which is partly obscured by rib fragments (Fig. 9). The humerus in ZMNH M8752 is rather straight, as is also the case in ZMNH M8728, whereas it appears curved in ZMNH M8727, which is probably attributable to its angle of preservation. The proximal head of the left humerus is incomplete; its minimal width at mid-shaft is 17 mm and its distal width is 30 mm. The length of the right humerus is 103 mm, but both its proximal and distal ends are not fully exposed, such that their width cannot be measured. An entepicondylar foramen is absent. The ectepicondylar groove, as well as the distal ectepicondylar notch, are weakly expressed. The left radius and ulna are very well preserved and exposed. Again, as in ZMNH M8728, the radius is somewhat more robustly built than the ulna. The radius shows marked expansions both proximally and distally, which result in a biconcave shaft, the postaxial margin of which is more deeply concave than the preaxial margin. The ulna is distinctly expanded proximally, but only weakly expanded distally. Its preaxial margin is concave, although less so than the postaxial margin of the radius. Together, the two elements define the spatium interosseum. The postaxial margin of the ulna is rather straight, yet damaged in its distal part.

Six carpal elements are ossified and preserved in the left manus. The proximal row of carpal elements of pentagonal circumference is preserved in articulation. Of those, the intermedium is the largest (maximum exposed length: 15.4 mm), followed by the radiale (15.2 mm) and the ulnare (14.3 mm). The distal carpal row comprises three ossifications of rounded contours, a large distal carpal 4 and smaller distal carpals 3 and 2. The metacarpals of the left manus are deflected away from the distal carpal ossifications and have been pushed up against one another, partially obscuring metacarpal V. Metacarpals I through to IV are all straight elements, with expanded proximal and distal ends and a biconcave shaft. Metacarpal V, well exposed in the right manus, is short and somewhat more massively built. Of all metacarpals, mcIII is the longest in the left manus, mcIV is the longest in the right manus and mcV is the shortest in both (Table 3).

Preservation of the phalanges is incomplete in the left manus. Digit II preserves two phalanges, digit III comprises two phalanges (a third one possibly lying atop a dorsal rib) and digit IV preserves three phalanges – evidently an incomplete count.

In the right forelimb, radius and ulna are partially obscured and crossing over each other. In the proximal carpal row, the radiale, intermedium and ulnare are identifiable yet less well preserved and exposed than in the left manus. The distal carpal ossifications cannot be located except for one that protrudes from below a phalanx. A total of nine disarticulated phalanges can be identified.

2.6.4. The pelvic girdle and hindlimb. As mentioned above, the sacral region is poorly preserved in ZMNH M8752, although two sacral vertebrae are identifiable. Neither ilium can be identified, but the ventral part of the left pubo-ischiadic plate is well preserved and exposed. It shows that, at least in their ventral parts, both the pubis and ischium are broad, plate-like ossifications, which meet each other for most of their depth in a suture. The thyroid fenestra is thus eliminated. The fact that this is not a primitive condition but a secondary development is indicated by the persistence of a small yet distinct cleft between pubis and ischium in the ventral margin of the pubo-ischiadic plate.

Both hindlimbs are preserved, but the left one is broken across the clustered segments of the proximal caudal vertebral column (Fig. 9). The femur is a rather straight element that is both proximally and distally expanded. Its preaxial (anterior) margin is at best only slightly concave, while the postaxial (posterior) margin is more distinctly concave. Like the other zeugopodial and stylopodial elements, the femur shows little morphological differentiation. The internal trochanter is not distinct and the articulation for tibia and fibula is continuous. The proximal end of the right femur is crushed and distorted.

The tibia and fibula are well preserved and exposed in the left hindlimb. The tibia is broadly expanded proximally, but less distinctly expanded distally. The shaft is biconcave, with the postaxial margin more deeply excavated than the preaxial margin. The proximal end of the tibia has straight pre- and postaxial margins, and its proximal margin is incomplete (broken). The fibula is only weakly expanded proximally, but it is very broadly

https://doi.org/10.1017/S175569102400001X

expanded distally. Its preaxial margin is deeply concave, its postaxial margin slightly convex. Together, the tibia and fibula define the spatium interosseum distal to which the astragalus is located.

The left tarsus comprises three ossifications of rounded contours. The astragalus, located distal to the spatium interosseum in an intermedium position, is the largest (maximum exposed length: 18.5 mm), followed by the calcaneum (17.5 mm) located distal to the fibula; the distal tarsal IV (11.6 mm) is located proximal to metatarsal IV (Table 5). All five metatarsals are beautifully preserved and exposed in the left foot. The first metatarsal is distinctly shorter than the other ones and almost of rectangular contours. All other metatarsals are straight elements with somewhat expanded proximal and distal ends and a biconcave shaft; there is no overlap of their proximal heads. Of all the metatarsals, mtIII is the longest. Other than the most proximal ones, the phalanges of the left foot are obscured by overlying caudal vertebrae. The right foot, broken across a proximal segment of the tail, allows a phalangeal count in the fourth digit only, which shows five phalanges (four phalanges and an ungual) – the primitive number.

2.7. Referred specimen, IVPP V20295

(Figure 11). This is the most complete and fully articulated specimen recovered to date. The skull is preserved in dorsal view and is in complete articulation with the neck and the rest of the body, which is essentially exposed on its left side. The total vertebral count is 145, comprising 32 cervical vertebrae, 30 dorsal vertebrae, 2 sacral vertebrae and 81 caudal vertebrae. It is estimated that the total length of the individual was approximately 521 cm and therefore just slightly longer than ZMNH M8752. Note that the incomplete holotype specimen IVPP V13767 represents the largest known individual of *Dinocephalosaurus orientalis*: its skull measures 23.06 cm in total length compared to 20.1 cm for IVPP V20295 and 17.01 cm for ZMNH M8752.

2.7.1. The skull and mandible. (Figure 12). The skull is 201 mm long and 108.7 mm wide across the temporal region as preserved. At the anteriormost end, the premaxillae have separated slightly along the midline. This is the result of dorsoventral compression of the skull, causing the anterior end to be somewhat splayed laterally. Clearly defined medial processes of the premaxillae extend posteriorly together over one third of the total length of the skull. The sutures marking the edges of the maxillae are clearly marked on both sides and are mirror images of each other. The sutures separating the nasals from the frontals and the parietal from the frontals are less clearly distinguishable, but they generally seem to follow the pattern in the holotype with interdigitating sutures. The presence of the distinctive narial gutters (antorbital recess) extending posteriorly from the external nares likewise mirrors the morphology of the holotype. The frontals are broad anteriorly where they meet the prefrontals, but they become noticeably constricted posteriorly, where they form the posterodorsal borders of the orbits. The frontals of most non-archosauriform archosauromorphs are also somewhat constricted in the interorbital region, with the notable exceptions of *Tanystropheus hydroides* and *Tanystropheus longobardicus*, in which the frontals are widened above the orbits, covering them

Figure 11 *Dinocephalosaurus orientalis* IVPP V20295. Complete articulated skeleton in dorsal to left lateral view. Abbreviations: ax = axis; ca.v = caudal vertebra; cv = cervical vertebra; do.v = dorsal vertebra; ga = gastralia; l.co = left coracoid; l.fe = left femur; l.hu = left humerus; l.il = left ilium; l.is = left ischium; l.ma = left manus; l.pes = left pes; l.pu = left pubis; l.ra = left radius; l.sc = left scapula; r.hu = right humerus; r.ca = right calcaneum; r.co = right coracoid; r.fi = right fibula; r.ma = right manus; r.ra = right radius; r.sc = right scapula; r.ti = right tibia; r.ul = right ulna.

https://doi.org/10.1017/S175569102400001X

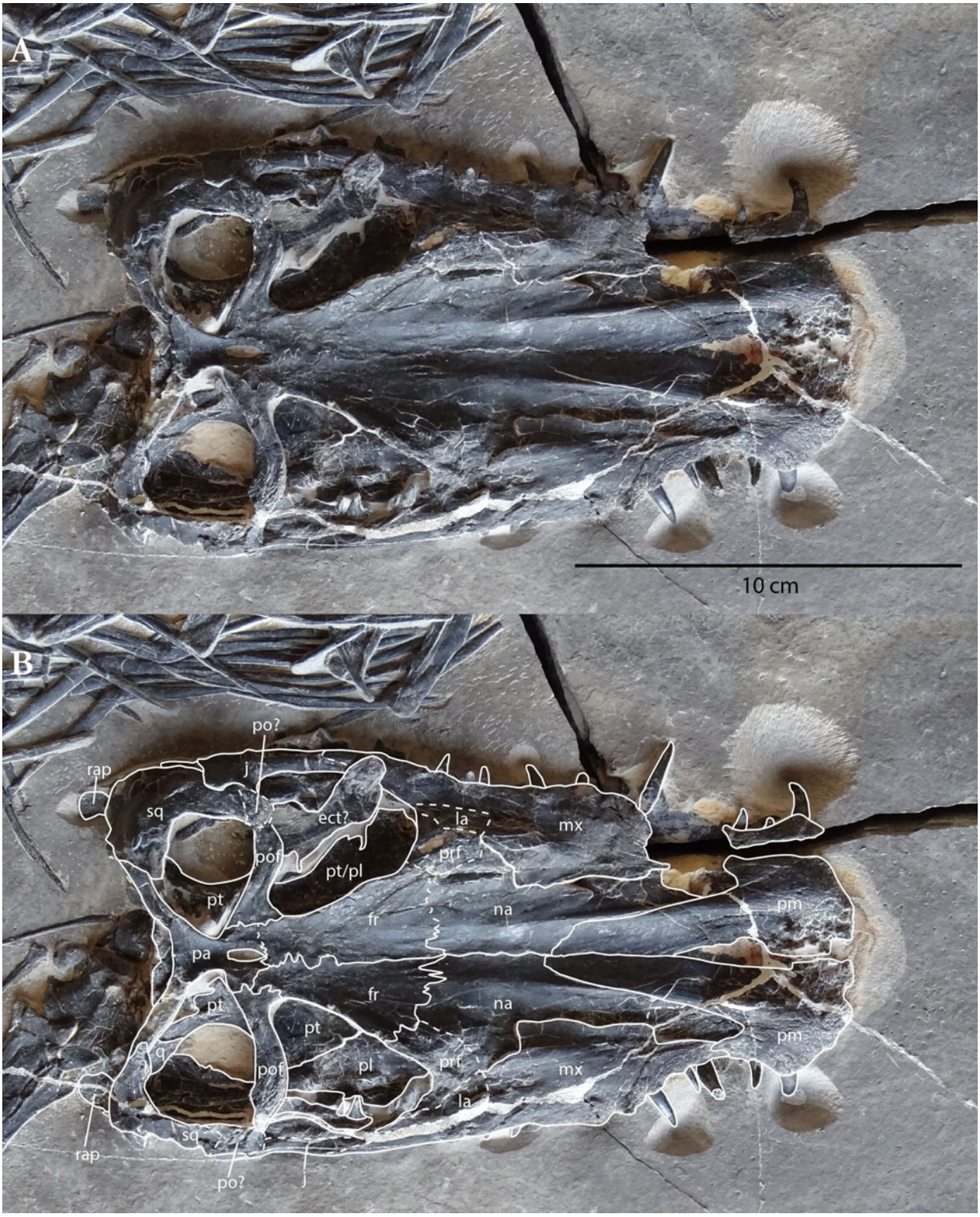

Figure 12 *Dinocephalosaurus orientalis* IVPP V20295. Detail of skull in dorsal view. (a) Photograph. (b) Photograph with interpretative drawing. Abbreviations: fr = frontal; la = lacrimal; mx = maxilla; na = nasal; pa = parietal; pl = palatine; pm = premaxilla; po = postorbital; prf = prefrontal; pt = pterygoid: rap retroarticular process.

dorsally (Nosotti 2007; Spiekman *et al*. 2020a, 2020b). There is a pronounced interdigitating median suture separating the frontals just anterior to the parietal. The parietal table is narrow, but flares posteriorly into the parietal 'wings' marking the posterior borders of the sub-circular supratemporal fenestrae. These parietal 'wings' are oriented posterolaterally as in most early archosauromorphs, except *Tanystropheus* spp., *Protorosaurus speneri* and *Azendohsaurus madagaskarensis*, which exhibit a lateral orientation of these processes (Gottmann-Quesada & Sander 2009; Flynn *et al*. 2010; Spiekman *et al*. 2020a). The prominent pineal foramen is of an elongate oval shape. A pineal foramen is generally present in most non-archosauriform archosauromorphs, although it is missing in *Macrocnemus* spp., *Trilophosaurus buettneri*, certain specimens of *Prolacerta broomi* and

https://doi.org/10.1017/S175569102400001X

the putative archosauromorph *Czatkowiella harae* (Spielmann *et al*. 2008; Borsuk-Białynicka & Evans 2009; Spiekman 2018; Miedema *et al*. 2020). The postfrontal is an elongated bone, oriented transversely relative to the longitudinal axis of the skull. On its medial end it articulates with the parietal on its posterior half and the frontal on its anterior half. This configuration corresponds with that of the holotype as outlined above (following the interpretation of Rieppel *et al*. 2008). As with the holotype skull, the strong dorsoventral crushing of the skull hampers observation of the relationship between the squamosal, postorbital and jugal. The postorbital in particular is badly broken and incomplete, and the dorsal portion of the jugal is also poorly preserved.

Parts of the palate can be observed in dorsal view through the orbit and supratemporal fenestra. On the right side a clear articulation is observed between the broad pterygoid and palatine, whereas the exact articulation between these elements is unclear on the left side. An additional disarticulated element is poorly preserved, but based on its relative position it might represent an ectopterygoid. Posteriorly, the articulation between the quadrate ramus of the pterygoid and the pterygoid wing of the quadrate is well preserved, with the latter overlapping the former laterally.

The two large 'fangs' seen on the maxilla of the holotype are not readily apparent in this new specimen, although the base of one such tooth has been exposed on the right side with the distal part extending into the matrix. The larger teeth develop striations towards the apex of the enamel crown, as in the other specimens. On the left side a break in the block has resulted in the loss of the posterior end of the premaxilla and the anterior portion of the maxilla. Nevertheless, each premaxilla is seen to bear at least one large tooth, and on the right side two similar teeth project up from the mandible. On the right side, two mandibular teeth can be observed through the orbit as a result of the deformation of the specimen. Two very weakly developed retroarticular processes can be seen behind the temporal region on both sides.

2.7.2. The vertebral column. (Table 4). The neural arch elements of the atlas are slightly displaced, but essentially the neck is in complete articulation with the skull. The first 22 cervical vertebrae flex around to form an almost complete circle with the tip of the snout before the series continues, passing backwards under the posterior region of the trunk immediately in front of the pelvis and straight back to the pectoral girdle. The cervical ribs of the first 17 cervical vertebrae have moved out of natural articulation with the individual vertebrae, lying in bundles just to one side of the neck. However, from cervical 18 onwards they are more closely articulated with their respective vertebrae.

In ZMNH M8728 (above) we noted a change in the form of the cervical vertebrae from a less concave ventral margin in lateral view together with an increase in the height of the neural spine at cervical 24. They also become shorter at this point. It would seem that this change in morphology might take place at vertebra 22 in IVPP V20295, although it should be noted that this is also exactly the region where the neck is overlain by the curled dorsal vertebrae and it is therefore somewhat difficult to assess this with complete confidence. Where the neck emerges from under the dorsal vertebrae, the vertebra (considered to be cervical vertebra 25) is very poorly preserved.

Cervical vertebra 27 has a neural spine that is much anteroposteriorly narrower and slightly taller than the preceding cervical vertebrae. The posteriormost cervical vertebrae (presacral vertebrae 28–32) together with the anterior dorsal vertebrae have

Table 4 Length and height of the sacral and caudal vertebrae, specimen IVPP V20295. Abbreviations: CAV = caudal vertebra; SV = sacral vertebra. The length was measured across the ventral margin of the centrum; the height was measured across mid-centrum and includes the neural crest. All measurements are in mm.

IVPP V20295								
Element	Length	Height	Element	Length	Height	Element	Length	Height
SV 1	31.7	–	CAV 27	–	–	CAV 55	16.9	22.4
SV 2	29	–	CAV 28	23.2	–	CAV 56	16.4	21.8
CAV 1	29.2	–	CAV 29	24.1	–	CAV 57	15.9	21.1
CAV 2	–	–	CAV 30	24.6	–	CAV 58	15.9	19.5
CAV 3	–	–	CAV 31	–	–	CAV 59	15.2	18.5
CAV 4	29.1	–	CAV 32	24.4	–	CAV 60	–	16.2
CAV 5	28.8	–	CAV 33	24.4	–	CAV 61	14.1	16.2
CAV 6	25.5	–	CAV 34	24	–	CAV 62	14	15
CAV 7	29	–	CAV 35	25.4	–	CAV 63	13.7	15.1
CAV 8	27.6	–	CAV 36	24.2	45.6	CAV 64	12	–
CAV 9	–	–	CAV 37	23.2	44.5	CAV 65	11.1	11.7
CAV 10	29.2	–	CAV 38	24.1	42.3	CAV 66	11	10
CAV 11	–	–	CAV 39	24	43.2	CAV 67	10	8.7
CAV 12	–	–	CAV 40	24.6	42.3	CAV 68	9.8	7.5
CAV 13	–	–	CAV 41	23.3	40.1	CAV 69	8.5	6.5
CAV 14	25.7	–	CAV 42	23.8	40.6	CAV 70	8.3	5.3
CAV 15	27.8	–	CAV 43	–	37.8	CAV 71	7.1	5.2
CAV 16	–	–	CAV 44	22.8	36.9	CAV 72	7	5
CAV 17	–	–	CAV 45	22.1	35.1	CAV 73	5.4	4.5
CAV 18	24.2	–	CAV 46	22.1	34.8	CAV 74	4.4	3.4
CAV 19	25.8	–	CAV 47	22.4	33.3	CAV 75	4.2	3.2
CAV 20	–	–	CAV 48	20.5	31.8	CAV 76	2.7	2.9
CAV 21	–	–	CAV 49	20.8	30.1	CAV 77	2.4	1.8
CAV 22	–	–	CAV 50	20.3	29.4	CAV 78	2.6	1.8
CAV 23	24.9	–	CAV 51	19.8	27.7	CAV 79	2.2	1
CAV 24	26.1	54.1	CAV 52	17.7	26.6	CAV 80	2.1	1
CAV 25	24.3	–	CAV 53	–	–	CAV 81	1.7	0.8
CAV 26	–	–	CAV 54	–	23.5			

https://doi.org/10.1017/S175569102400001X

characteristic neural spines that take the form of a relatively narrow backward-pointing hook. The transition to the dorsal vertebrae seems to be partially marked by this neural spine having a slight anterior projection or knob (forming a weak T-shape in lateral view). Whereas all the preceding cervical ribs have a clear anterior process and a posteriorly curving shaft, the rib of presacral vertebra 32 is transitional; it lacks an anterior process and its shaft is straight but posteroventrally directed, relatively short, and with a blunt distal end. Since this rib is considerably shorter than the subsequent dorsal ribs and does not seem to contribute to the dorsal rib cage, its corresponding vertebra is identified as the posteriormost cervical, as in ZMNH M8728.

In contrast to *Tanystropheus hydroides*, the neck of *Dinocephalosaurus orientalis* is often preserved strongly flexed, and in IVPP V20295 the neck is coiled to the extreme. As in other specimens, many of the ribs have 'popped out' of position – not flexed nor broken, so that they retain their long straight shafts. This may simply be because of the relatively shorter but greater numbers of vertebrae allowing the neck to flex postmortem. It is very unlikely that the neck was so flexible in life. The ribs certainly maintain a straight position with no major flexion. Although the rib heads may have been displaced away from the vertebral column, they still remain very much aligned with their respective vertebrae – they have moved relatively little forward or backward from the positions in life. This is perhaps indicative of these splayed ribs being encased by skin at the time of burial. On the other hand, although shorter than in *Tanystropheus* in absolute terms, they do traverse a greater number of intervertebral joints – five is a typical number crossed – which in the absence of any dewlap would suggest a degree of rigidity from these bundles of ribs.

The first six dorsal vertebrae are slightly out of articulation with each other and describe a tight radius. There is then a small break followed by the remaining dorsal vertebrae that complete the circular disposition of the body. There are either 29 or 30 dorsal vertebrae depending on which vertebra is considered the first sacral, but 30 is considered the most likely.

Where the posteriormost cervical and anteriormost dorsal vertebrae lie alongside the proximal tail, the vertebrae are rather poorly preserved and the bone surface is very fragmented. The same condition also pertains to most of dorsal vertebrae 5–15, as well as sections of the caudal vertebrae including those situated alongside the first two dorsal vertebrae.

The neural spines of all the dorsal vertebrae are relatively small and narrow, but expand distally into a low, rugose ridge, so that they are broadly T-shaped in lateral view. As in all other specimens, the anterior dorsal vertebrae (1 through to approximately 12) have very distinctive and well developed transverse processes with a deeply excavated anterior surface and a concomitantly markedly convex posterior edge. They are also very tall and narrow. In the region of dorsal vertebra 13 or 14 the height of the transverse process is somewhat reduced and the diapophysis becomes more prominent and circular. This reduction in height and development of a more circular facet for the rib continues to the sacral vertebrae.

For the most part the dorsal ribs lie disarticulated from the vertebrae, but still in close association. They are all single-headed, but anteriorly they have deeper heads with what could be described as a more robust tuberculum portion that extends ventrally into a narrow and elongate capitulum region. In the more posterior ribs, the heads become more rounded, corresponding to the reduction in complexity of the transverse processes.

The short transverse processes on vertebrae 60–63 are quite pronounced, with those on 61 and 62 being the largest, and which we regard here as the two sacral vertebrae. Yet at first glance vertebrae 61 and 62 also seem to have associated 'haemal spines', which is hard to reconcile. However, on closer inspection, it is clear that these 'haemal spines' have exceptionally anteroposteriorly flared distal rami and it is almost certain that they represent sacral ribs that have been displaced, in turn indicating that they were not fused to the sacral vertebrae. These ribs are also consistent with the element thought to be a sacral rib overlying the top edge of the left ilium. If they are sacral ribs then there are only four preserved, which in turn is indicative of just two sacral vertebrae, the number present in all known non-archosauriform archosauromorphs. Equally, it does not appear as though both ribs could articulate with the ilium, as the iliac blade is so reduced (see below). Vertebra 63 also has a broad and prominent facet on the end of a short transverse process, but it must be assumed to be the first caudal. It would have been impossible for the associated rib to have made any contact with the pelvis.

The left femur partially covers the neural spines of the last dorsal, both sacral and the anteriormost caudal vertebrae. In addition, the left fibula partially obscures the second caudal, so it is not possible to state unequivocally whether there is a distinct change in the nature of the neural spines between the dorsal vertebrae, sacral vertebrae and caudal vertebrae. However, from what is exposed of these elements, it would appear that both sacral vertebrae have relatively tall neural spines that are rectangular in lateral view, a condition shared with the anterior caudal vertebrae. This contrasts with the somewhat 'waisted' (or weakly T-shaped) appearance of the preceding dorsal neural spines terminating in a distinctly rugose surface.

It is difficult to measure the dimensions of the dorsal vertebrae (Table 4) because of the way the torso curls around on itself and the ribs overlap the vertebrae, but dorsal vertebrae 6 and 7 (although distorted) are clearly exposed and provide potentially useful reference points for other specimens, as does dorsal vertebra 20.

The tail is preserved completely intact and fully articulated with a complement of 81 vertebrae. The mid to distal tail is beautifully exposed, and displays the remarkable hatchet-shaped chevrons mirroring the rounded neural processes. The first haemal arches are quite broad-based and occur in the first two caudal vertebrae. At least the first ten – if not more – caudal vertebrae have a 'typical' rectangular neural spine and chevron bones. The transition to the hatchet-shaped form appears to begin at around caudal 16, although bones of the pectoral girdle obscure part of the tail in this region. The chevrons become much shallower and more elongate at caudal 44, and there is also a change in shape, so that the ventral edge is convex in lateral view. At about the same point there is also a noticeable shift in the shape of the neural spines so that they are more inclined posteriorly and more clearly expressed on the posterior half of the vertebra. The chevrons and neural spines progressively diminish in size but the chevrons can still be clearly distinguished as separate elements even as far posteriorly as caudal 75, where the centra is a mere disc of bone.

The gastralia are loosely associated and extend from about the sixth dorsal vertebra back as far as the sacrum. As in other specimens, they display two different morphologies: the medioventral elements that are slightly angulated and the collateral elements that terminate in a blunt tip proximally and a slender tapering tip distally.

2.7.3. The pectoral girdle and forelimb. Both pectoral girdles and forelimbs are almost intact and only partially disarticulated. The left limb and girdle lie a short distance from the vertebral column and are missing the proximal head of the humerus and the glenoid portion of the coracoid. The right pectoral girdle is also displaced from its natural position and lies partially under the dorsal ribs (the scapula) and over the proximal tail (the coracoid) where it coils around the body. Both the scapula and

https://doi.org/10.1017/S175569102400001X

Figure 13 *Dinocephalosaurus orientalis* IVPP V20295. Detail of left hindlimb as preserved. Abbreviations: as = astragalus; ca = calcaneum; fe = femur; fi = fibula; il = ilium; mt = metatarsal; pu = pubis; sa.r = sacral rib; ti = tibia.

coracoid are kidney-shaped elements of approximately equal size, the scapula just marginally larger in the development of the posterodorsally projecting scapular blade. The posterior margin of the coracoid is deeply notched below the level of the glenoid fossa, and there is a distinct coracoid foramen. Neither interclavicle nor clavicles are preserved.

The humeri and epipodials are all columnar elements with minimal development of the proximal and distal heads. The left radius almost completely overlies the left ulna, and in the right limb the radius is also out of position. The arrangement of carpals is difficult to discern as both wrists overlap. Nevertheless, there is a total of 12 circular carpals and therefore presumably a total of six in each wrist. As preserved in the left forelimb the phalangeal formula is 1:2:3:5:1 (Table 3), but the terminally preserved hourglass-shaped phalanges are similar in form to all the other phalanges and are not spatulate or claw-shaped as might be expected for unguals. The right forelimb is a bit disrupted where it extends over the left forelimb, and digits 1 and 2 are disassociated. However, digit 3 bears three phalanges, digit 4 has six phalanges, with the terminal one being expressed as a small round disc, and in digit 5 just a single phalanx is preserved. Thus, it would seem that terminal phalanges fail to ossify in this taxon.

2.7.4. The pectoral girdle and hindlimb. (Figure 13) Of all the specimens of *Dinocephalosaurus orientalis* described here, the elements of the pelvis are the most clearly displayed in IVPP V20295. There is no definitive embayment constituting the thyroid fenestra between the pubis and ischium, although there was almost certainly a deep notch along the articulation between the two towards the median symphysis.

The three elements of the left pelvic girdle have separated slightly from each other, with the ischium and ilium almost in their original position relative to each other. The pubis has been pushed forward slightly by the intervention of the right femur and ischium. The pubis is an almost circular element that is slightly larger than the ischium. It bears a rugose area on its dorsal margin that articulated directly with the ilium. The ischium is of an approximate trapezoidal shape with the posterior margin being slightly convex, resulting in a very weak posterior process. The left ilium is complete but the small dorsal process is partially covered by the second sacral rib. This dorsal process is not developed anteriorly at all (i.e., a preacetabular process is completely absent) but has a short, poorly developed posterior projection (i.e., a postacetabular process). The acetabulum is shallow and the acetabular contribution of the ilium is semi-lunate shaped.

The right ilium is not obviously visible, but it is probably covered by the left pubis. A short section of bone extending between the left pubis and left ilium apparently represents a short section of the dorsal process of the right ilium. The right pubis lies just anterior to its left counterpart. It displays a weakly developed bony strut extending anteroventrally from the margin of the acetabulum. The right ischium is draped over and closely oppressed to the proximal half of the femur, such that the boundaries of the femur can be clearly distinguished through the plate-like ischium. The anterior margin is a little fragmented and the posterior margin is covered by the left ischium so that it adds nothing further to the description.

The right hindlimb is almost in full articulation so that the proximal head of the femur appears to be resting within the acetabulum, although it is covered by the ischium. The left femur preserves a clear internal trochanter, which is proximodistally straight. Proximally, the trochanter does not quite reach the proximal end of the femur. The femur is a robust, relatively straight element, and the tibia is the more robust of the two columnar epipodials, which bow away from each other to leave a prominent spatium interosseum as in all other specimens. The only tarsal elements preserved are the astragalus and calcaneum, and these are simple rounded discs that are not in contact with each other. There is a noticeable gap between the proximal carpals and the metatarsals, strongly implying that distal carpals were not ossified.

Unfortunately, the distal end of digit 3 is missing on the block, but the other four digits would appear to be complete. If so, this gives the rather unusual formula of 1:2:?:2:1 with the third digit having a minimum of three phalanges (Table 5). The left

https://doi.org/10.1017/S175569102400001X

Table 5 Length and width of hindlimb elements in the two specimens preserving the hindlimbs, ZMNH M8752 and IVPP V20295. Abbreviations: L = length; PW = proximal width; MW = minimal width; DW = distal width. All measurements are in mm.

		ZMNH M8752	IVPP V20295
Left femur	L	~111.0	126.1
	PW	–	34.2
	MW	13.0	17.3
	DW	30.0	32.4
Right femur	L	~110.0	–
	PW	36.0	–
	MW	13.3	15.4
	DW	23.3	31.7
Left tibia	L	62.5	72.5
	PW	23.3	25.9
	MW	11.2	15.5
	DW	18.1	16.9
Right tibia	L	59.5	70.4
	PW	24.9	–
	MW	12.5	13.7
	DW	18.8	18.2
Left fibula	L	–	81.8
	PW	~13.0	–
	MW	10.1	–
	DW	28.1	–
Right fibula	L	–	–
	PW	–	16.7
	MW	–	–
	DW	–	30.2
Left metatarsal I	L	15.3	–
Right metatarsal I	L	–	22.2
Left metatarsal II	L	26.9	–
Right metatarsal II	L	26.4	35.6
Left metatarsal III	L	35.5	–
Right metatarsal III	L	34.0	42.0
Left metatarsal IV	L	34.1	–
Right metatarsal IV	L	33.6	42.9
Left metatarsal V	L	25.4	–
Right metatarsal V	L	–	31.9

hindlimb is more disarticulated with the femur and epipodials draped over the proximal tail, although the fibula is deflected away from the tibia distally. The astragalus and calcaneum lie on top of the neural spines of the sixth and seventh caudal vertebrae, and the digits extend backward below the tail. However, only three digits are clearly exposed. The longest digit (likely digit 3) has six phalanges including a blunt spatulate-shaped terminal phalanx.

2.7.5. Remains in the abdomen. (Figure 14). Within the body cavity in the mid-dorsal region lie the remains of a minimum of four fishes. Their scales clearly overlap the right ribs, but are under the left ribs. At least one of these fishes, the most complete, can be referred to the genus *Lashanichthys*, a holostean. In addition, two partially preserved specimens lying close by, probably belong to the same taxon. A larger specimen with distinct ganoid scales is possibly a member of the genus *Colobodus*, which is known from Panxian (currently known as Panzhou) (e.g., Sun *et al*. 2008). Further posteriorly, there are remains of a number of small vertebral elements and a possible limb bone. These could conceivably represent an embryo, or alternatively are the remnants of a small prey reptile, but their identities remain equivocal. The three most complete of the tiny vertebrae lie on top of the 23rd cervical. One has a distinct and quite broad neural spine that is perhaps not entirely consistent with any of the *Dinocephalosaurus* vertebrae apart from the axis. The limb element is a straight shaft with no distinct enlargement of either end and is 26.6 mm long.

3. Discussion

Liu *et al*. (2017) referred the Luoping specimens to *Dinocephalosaurus* sp. While they did note the existence of 'slight differences', they felt that the incomplete nature of the available material was insufficient to demonstrate consistent differences between specimens from the two different locations (Liu *et al*. 2017: page 3). We note that LPV 30280 is the smallest of all the specimens referred to *Dinocephalosaurus*. LPV 30280 is particularly

Figure 14 *Dinocephalosaurus orientalis* IVPP V20295. Detail of gut contents (fishes) in gastral region. On the left is a complete specimen of *Lashanichthys* sp. and on the right a partial specimen referred to *Colobodus* sp.

https://doi.org/10.1017/S175569102400001X

noteworthy for the description of a partial embryo in the abdominal region (Liu *et al*. 2017). Although incomplete, these remains are certainly consistent with them being referable to *Dinocephalosaurus* sp., and therefore evidence of viviparity in this form. This in turn demonstrates sexual maturity in this small individual, which may constitute possible evidence of taxonomic differences or sexual dimorphism between LPV 30280 and the larger specimens described herein. However, the incompleteness of LPV 30280 makes further speculation simply that.

Despite extensive sampling during close to three centuries, unequivocal remains of *Dinocephalosaurus orientalis* or closely related taxa have not been discovered from the western Tethys (i.e., Europe and the Middle East). However, the excellent preservation of the here newly described material of *Dinocephalosaurus orientalis* allows for a re-evaluation of certain enigmatic, isolated remains from the Germanic Basin. In particular, jaw remains attributed to *Lamprosauroides goepperti*, a taxon that is currently considered a *nomen dubium* (Rieppel 1995), exhibit a morphology that is remarkably similar to that of *Dinocephalosaurus orientalis*. *Lamprosauroides goepperti* is known from two isolated maxillae from the Lower Muschelkalk of Krapkowice and Gogolin in Upper Silesia, Poland, whereas a single, isolated dentary from the Lower Muschelkalk of Winterswijk in the Netherlands was recently attributed to cf. *Lamprosauroides goepperti* (Spiekman & Klein 2021). Like *Dinocephalosaurus*, the dentition of *Lamprosauroides* is composed of slender, slightly recurved teeth anteriorly, and wider, straight teeth in the middle and posterior sections of the jaw, which only possess striations on the distal half of the crown. And like *Dinocephalosaurus*, the two maxillae referred to *Lamprosauroides* also have a sinusoidal outline of the tooth row, and they both possess two enlarged, fang-like teeth in what are possibly the fourth and fifth tooth positions. Finally, the presence of plicidentine, which is present in *Dinocephalosaurus*, was also confidently established in the lower jaw from Winterswijk. The presence of dinocephalosaurids in the western Tethys would corroborate previous findings that suggest a close similarity between the faunas of the eastern and western Tethys regions (e.g., Li 2007; Rieppel *et al*. 2010; Jaquier *et al*. 2017). However, the material of *Lamprosauroides* is very fragmentary, and it also shows distinct similarities with (possibly cymatosaur) eosauropterygians (Rieppel 1995; Spiekman & Klein 2021). Therefore, there is currently insufficient evidence to assign this material to *Dinocephalosaurus orientalis*, nor to convincingly indicate the presence of dinocephalosaurids in the Germanic Basin. Nevertheless, the discovery of new taxa from the eastern Tethys represented by articulated specimens clearly merits the re-evaluation of isolated remains from historical European collections.

3.1. Phylogeny

3.1.1. Methods. The new morphological information for *Dinocephalosaurus orientalis* has been incorporated into a detailed phylogenetic character data matrix focusing on the interrelationships of non-crocopodan archosauromorphs. This matrix was first presented by Spiekman *et al*. (2021), and has subsequently been applied and modified by Wang *et al*. (2023). Based on the new findings, 12 characters have been modified and several character scorings have been updated relative to the most recent iteration of the matrix (Wang *et al*. 2023), including 88 character state modifications for *Dinocephalosaurus orientalis*. These modifications, as well as an updated version of the character list and character matrix, can be found in the supplementary material available at https://doi.org/10.1017/S175569102400001X.

The matrix was analysed using TNT 1.5 (Goloboff & Catalano 2016). Following the methodology of Spiekman *et al*. (2021), the problematic operational taxonomic units (OTUs) *Czatkowiella harae*, *Tanystropheus 'conspicuus'* and *'Tanystropheus antiquus'* were excluded *a priori* from the analysis. Ratio characters are included and the characters indicated as ordered (= additive) in the character list were treated as such, corresponding to analysis 4 of Spiekman *et al*. (2021). Characters 1, 2, 4, 5, 7, 9, 13, 35, 43, 62, 73, 77, 78, 83, 84, 88, 89, 110, 114, 118, 128, 136, 140, 144, 153, 158, 159, 162, 178, 185, 187, 194, 195, 200, 205, 209, 219, 220, 224, 230, 232, 242, 248, 251, 258, 259, 264, 267, 276, 292, 294, 297, 298, 299 and 305 were thus treated as additive. Tree searches were conducted under equal weights using a traditional search that included 1,000 Wagner trees replications with random addition sequence and TBR branch swapping holding ten trees per replicate. Values of Bremer and bootstrap support were calculated for the equal weight analysis, with the latter being conducted using a traditional search with 1,000 iterations. Following the methodology of Spiekman *et al*. (2021), the iterative PCR protocol implemented in TNT (Pol & Escapa 2009) was used to identify an unstable OTU in the analysis and to exclude this taxon from the strict consensus tree (SCT). This resulted in a more resolved reduced strict consensus tree (RSCT), which allows easy assessment of the relationships of taxa that are obscured by the unstable OTU in the SCT.

3.1.2. Results. The updated phylogenetic analysis recovers *Dinocephalosaurus orientalis* and *Pectodens zhenyuensis* within a monophyletic Dinocephalosauridae, which forms the sister clade to Tanystropheidae in all most parsimonious trees (MPTs) (Fig. 15a). This contrasts with the results of the same analysis in both Spiekman *et al*. (2021: analysis 4, fig. 36a) and Wang *et al*. (2023), in which the position of Dinocephalosauridae relative to Tanystropheidae, *Prolacerta broomi* and Crocopoda was unresolved in the SCTs. The exact composition of Tanystropheidae, which is defined as 'The most recent common ancestor of *Macrocnemus*, *Tanystropheus*, and *Langobardisaurus* and all of its descendants' (Dilkes 1998), is unclear based on the SCT, since a polytomy is formed by *Fuyuansaurus acutirostris*, *Augustaburiania vatagini*, a clade composed of *Macrocnemus* spp. and *Elessaurus gondwanoccidens*, and a clade composed of all remaining tanystropheids. The iterative PCR protocol identified *Augustaburiania vatagini* as an unstable OTU and the resulting RSCT found *Fuyuansaurus acutirostris* outside Tanystropheidae as its sister taxon (Fig. 15b). The relationships within Tanystropheidae have also changed relative to previous iterations of this analysis (Spiekman *et al*. 2021; Wang *et al*. 2023). *Elessaurus gondwanoccidens* is now found as the sister taxon to *Macrocnemus obristi* within a clade also composed of *Macrocnemus bassanii* and *Macrocnemus fuyuanensis*. In the RSCT, the *Macrocnemus* spp. + *Elessaurus gondwanoccidens* clade forms the sister group to all remaining tanystropheids. Within this more inclusive tanystropheid clade, *Ozimek volans* and *Amotosaurus rotfeldensis* are recovered as sister taxa, and a large polytomy is found that comprises *Gracilcollum latens* (Wang *et al*. 2023), *Tanytrachelos ahynis*, AMNH FARB 7206, *Langobardisaurus pandolfii*, *Sclerostropheus fossai*, and a clade composed of *Tanystropheus* spp. and *Raibliania calligarisi*, in which the latter is found as the sister taxon to *Tanystropheus longobardicus*. Outside Tanystropheidae, the position of *Jesairosaurus lehmani* and the relative positions of *Prolacerta broomi*, Tanystropheidae, Dinocephalosauridae and Crocopoda differ from those seen in analysis 4 of Spiekman *et al*. (2021) and that of Wang *et al*. (2023) Rather than being the sister taxon to Dinocephalosauridae, *Jesairosaurus lehmani* is recovered at the very base of Archosauromorpha as the sister taxon to all other archosauromorphs, similar to analysis 3 of Spiekman *et al*. (2021: fig. 35). *Prolacerta broomi* forms the sister taxon to a clade comprising Crocopoda + Dinocephalosauridae + Tanystropheidae, again similar to analysis 3 of Spiekman *et al*. (2021). The interrelationships within Crocopoda remain

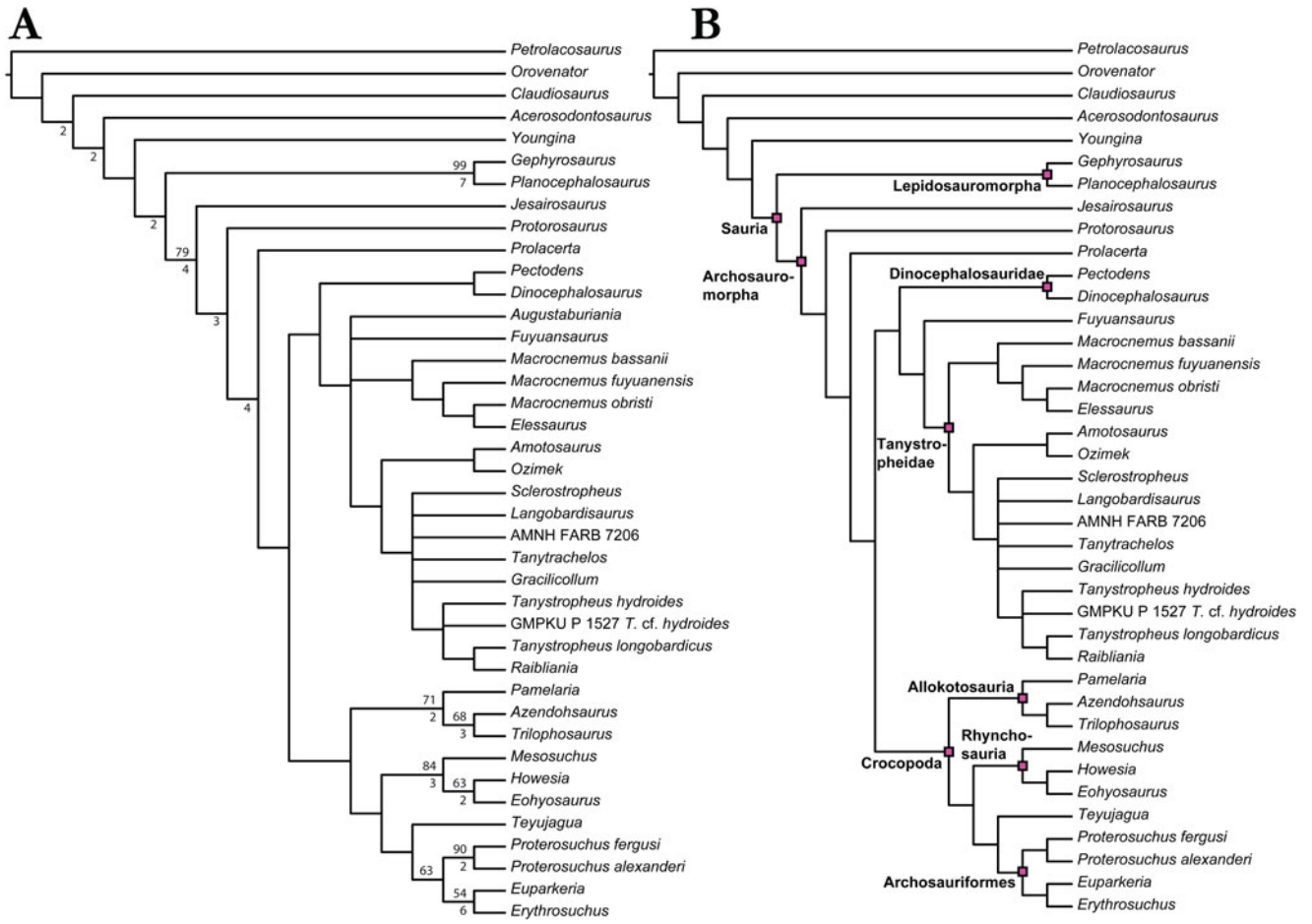

Figure 15 Cladograms of the phylogenetic analysis. (a) SCT of eight trees of 1,240 steps. Bremer values above 1 and bootstrap frequencies above 50% are provided above and below each node, respectively. (b) RSCT after the exclusion *a posteriori* of *Augustaburiania vatagini*, which has gained one additional node relative to the SCT.

unchanged relative to analysis 4 of Spiekman *et al*. (2021) and that of Wang *et al*. (2023).

3.1.3. Discussion. The results of our analyses corroborate previous analyses (e.g., Liu *et al*. 2017; De Oliveira *et al*. 2020; Spiekman *et al*. 2021) that suggest that *Dinocephalosaurus orientalis* represents a non-crocopodan archosauromorph (i.e., the paraphyletic grouping which, among others, includes *Protorosaurus speneri*, *Jesairosaurus lehmani*, tanystropheids and possibly *Prolacerta broomi*; Ezcurra 2016; Spiekman *et al*. 2021). As in previous iterations of this analysis (Spiekman *et al*. 2021 and Wang *et al*. 2023), it is found within a monophyletic Dinocephalosauridae, but this clade is now recovered as the sister clade to *Fuyuansaurus acutirostris* + Tanystropheidae. Support values among dinocephalosaurids and tanystropheids in our analysis are low, with bootstrap support under 50% and Bremer support values of one for all nodes in this part of the tree. Only a single additional step is required to force *Dinocephalosaurus orientalis* and *Pectodens zhenyuensis* within Tanystropheidae. When *Dinocephalosaurus orientalis* and *Pectodens zhenyuensis* are constrained within Tanystropheidae, the resulting analysis is highly unstable, with 278 recovered MPTs, but *Dinocephalosaurus orientalis* and *Pectodens zhenyuensis* both generally recovered deeply nested within Tanystropheidae. Other recent analyses have found *Dinocephalosaurus orientalis* to form the sister taxon to tanystropheids (Liu *et al*. 2017) or in a clade with *Jesairosaurus lehmani*, which together formed the sister clade to all other archosauromorphs (De Oliveira *et al*. 2020). Note that both *Pectodens zhenyuensis* and *Fuyuansaurus acutirostris* were not included in either analysis.

In general, tanystropheid and dinocephalosaurid phylogeny is strongly hampered by widespread homoplasy, particularly when it comes to cervical morphology, as has been recently outlined in detail (Wang *et al*. 2023). Consequently, the phylogenetic position of other, more enigmatic forms that also possess particularly long necks or elongate cervical vertebrae, such as *Sclerostropheus fossai* and *Gracilicollum latens*, remains highly ambiguous. The only known specimen of *Gracilicollum latens* comprises a poorly preserved skull and partial cervical column, and therefore comparatively few phylogenetic characters can be scored for this taxon. Certain features, such as the presence of a dentition indicating a piscivorous diet and a large number of cervical vertebrae (>18), might suggest this taxon is actually closely related to *Dinocephalosaurus orientalis*, rather than the tanystropheid affinity currently recovered. As has been noted previously (Wang *et al*. 2023), more specimens of *Gracilicollum latens* are probably required to more confidently assess its phylogenetic affinities. The extremely long-necked *Raibliania calligarisi* is recovered as the sister taxon of *Tanystropheus longobardicus* within a *Tanystropheus* spp. clade. This result is unsurprising considering the postcranial morphology of *Raibliania calligarisi*, which is very similar to that of *Tanystropheus longobardicus* (Dalla Vecchia 2020). No cranial material other than a disputed tooth is known for *Raibliania calligarisi*, but this taxon can probably be referred to the genus *Tanystropheus*. *Elessaurus gondwanoccidens* is found nested within a *Macrocnemus* spp. clade. This taxon is represented only by a largely complete hindlimb and a partial pelvis, sacrum and anterior caudal vertebrae (De Oliveira 2020), and it can currently only be distinguished from

https://doi.org/10.1017/S175569102400001X

Macrocnemus spp. by the relative proportions of its hindlimb and pes, as well as by possessing a femur with a lateral condyle that projects further distally than the medial condyle (ch. 282) and the absence of a posterior groove on the astragalus (ch. 290). Currently, insufficient information is available to confidently ascertain the relationship of this taxon relative to *Macrocnemus* spp. and tanystropheids generally.

Certainly, *Dinocephalosaurus orientalis* and *Tanystropheus* spp. largely independently achieved a comparable and impressive degree of neck elongation (Li *et al*. 2004). In *Tanystropheus* spp., this is achieved primarily through elongation of the length of individual cervical vertebrae, with the neck being composed of only 13 cervical vertebrae (Wild 1973; Nosotti 2007; Rieppel *et al*. 2010), whereas in *Dinocephalosaurus orientalis* the elongation of the individual vertebrae is more modest (Wang *et al*. 2023), but the number of cervical vertebrae is dramatically increased to 32. Nevertheless, due to the poorly constrained phylogeny of tanystropheids and dinocephalosaurids, the possibility that both taxa are more closely related than currently considered cannot be excluded. Consequently, an initial elongation of the neck, achieved either through limited elongation of individual vertebrae or a small increase in cervical number, or a combination of both, could have occurred in a common aquatic ancestor that both taxa shared to the exclusion of terrestrial tanystropheids like *Macrocnemus* spp. and *Langobardisaurus pandolfii*.

Interestingly, *Dinocephalosaurus orientalis* and *Tanystropheus* spp. also share several other features besides neck elongation to the exclusion of most other tanystropheids. These include, among others: a reduction in the number of premaxillary and maxillary teeth (chs. 13 and 26), the presence of a fish-trap type dentition (ch. 165), the presence of striations on marginal dentition (ch. 173, also present in *Gracilicollum latens*), the absence of a constriction on the ventral margin of the ischium (ch. 278) and the absence of a pedal centrale (ch. 291). It is apparent that many of these features probably represent adaptations to an aquatic environment, such as dental traits related to diet, altered limb proportions, a reduction in complexity in pelvic girdle morphology and the number of carpal and tarsal ossifications, which represent paedomorphic features that widely occur in aquatic reptiles (Rieppel 1989; Chen *et al*. 2014).

In addition to this, *Dinocephalosaurus orientalis* shares a remarkable set of cranial features with *Tanystropheus hydroides* (Fig. 16), which are absent or considerably less well developed in the smaller-sized *Tanystropheus longobardicus* and other tanystropheids: the presence of an antorbital recess (ch. 33), fused parietals (ch. 74), an absence of teeth on the palatine and anterior ramus of the pterygoid (ch. 100), a large and anteriorly rounded anterior ramus of the pterygoid (ch. 108) and the presence of a keel on the anterior end of the dentary (ch. 146). It seems likely that at least some of these features represent adaptations to the piscivorous, aquatic lifestyle that these two taxa share. In contrast, the diet of *Tanystropheus longobardicus* probably consisted of soft-shelled invertebrates (Spiekman *et al*. 2020a).

However, *Dinocephalosaurus orientalis* also possesses several features that differentiate it, together with *Pectodens zhenyuensis*, from all or most tanystropheids, including *Tanystropheus hydroides*. These character states include: the presence of a prenarial process of the premaxilla (ch. 7), the absence of a posterior process of the jugal (ch. 42, shared with *Amotosaurus rotfeldensis*), a ratio of the length of the ventral process of the postorbital versus the length of the posterior process of the postorbital less than 1.0 (ch. 62), postaxial cervical vertebrae without a transverse expansion of the neural spine (ch. 180), posterodorsally inclined neural spines of the anterior to mid-postaxial cervical vertebrae (ch. 194), holocephalous anterior dorsal ribs (ch. 213), a ratio of the longest metacarpal versus the longest metacarpal of 0.6 (ch. 258) and a relatively elongate, straight metatarsal V (chs. 300 and 305). Although it cannot be assumed *a priori* that these shared character states are not homoplastic between *Dinocephalosaurus orientalis* and *Pectodens zhenyuensis*, they are highly unlikely to represent convergences related to lifestyle, given the large size discrepancy and marked difference in dentition and general body plan between the two taxa.

Our outcome corroborates previous analyses (Liu *et al*. 2017; De Oliveira *et al*. 2020; Spiekman *et al*. 2021) that *Dinocephalosaurus* and *Tanystropheus* are most likely relatively distantly related taxa among non-crocopodan archosauromorphs and that their close morphological similarities (highly elongated neck, skeletal paedomorphosis and shared cranial features including fish-trap type dentition and narial recess) were acquired convergently, highlighting the high evolutionary diversity of non-archosauriform archosauromorphs within 10 million years of the Permo-Triassic extinction event.

3.2. Lifestyle

It is remarkable that within one group of tetrapods (non-crocopodan archosauromorphs) the excessive elongation of the neck (Fig. 16d) should be achieved convergently in quite different ways. Does the increased number of cervical vertebrae in *Dinocephalosaurus orientalis* compared to *Tanystropheus* spp. confer more mobility of the neck? At first, this does not seem likely as the cervical ribs extend across a number of intervertebral joints and are bundled together underneath the cervical column. The same configuration has previously been suggested to have provided strength and rigidity to the neck in *Tanystropheus* spp. (Tschanz 1986). Histological sectioning of the cervical ribs of *Tanystropheus* sp. indet. has shown that they are primarily composed of lamellar bone rather than being formed by ossified tendons as in, for instance, sauropod dinosaurs (Jaquier & Scheyer 2017). This suggests that the cervical ribs were indeed stiffened structures that were well developed to provide strength and rigidity to the cervical column. Although it has so far not been possible to conduct such an analysis on the cervical ribs of *Dinocephalosaurus* due to the rarity of the material, it is likely that they had a similar developmental origin and function, since elongated cervical ribs are widespread among non-crocopodan archosauromorphs (Spiekman *et al*. 2021). *Dinocephalosaurus orientalis* also shares the presence of dorsoventrally very low neural spines of the cervical vertebrae with *Tanystropheus* spp., as well as with *Pectodens zhenyuensis* and several (other) tanystropheids. Tschanz (1986) previously suggested for *Tanystropheus* that this would severely limit accommodation for epaxial musculature, thus limiting dorsoventral flexion of the neck. However, it is important to note that modern quantitative biomechanical testing of neck flexibility is lacking for both *Tanystropheus* and *Dinocephalosaurus*, and this could provide important new insights into the cervical flexibility of these long-necked taxa.

What evolutionary advantage these extraordinary long necks might have conferred is difficult to imagine. Li *et al*. (2004) postulated that the long neck together with the arrangement of the cervical ribs might confer an ability to employ an unusual suction feeding strategy, which would require deflection of the cervical ribs in a different functional context from the one outlined above. However, as has also been outlined by Spiekman *et al*. (2020b) for *Tanystropheus hydroides*, the fish-trap type dentition of *Dinocephalosaurus orientalis*, which is functionally equivalent to that of *Tanystropheus hydroides*, negates the possibility of suction feeding, since the long and curved teeth prevent the prey from entering the buccal cavity in such a scenario. Also, as has similarly been described for *Tanystropheus hydroides*, no heavily ossified hyobranchial apparatus is known for *Dinocephalosaurus orientalis*, despite the availability of several highly

https://doi.org/10.1017/S175569102400001X

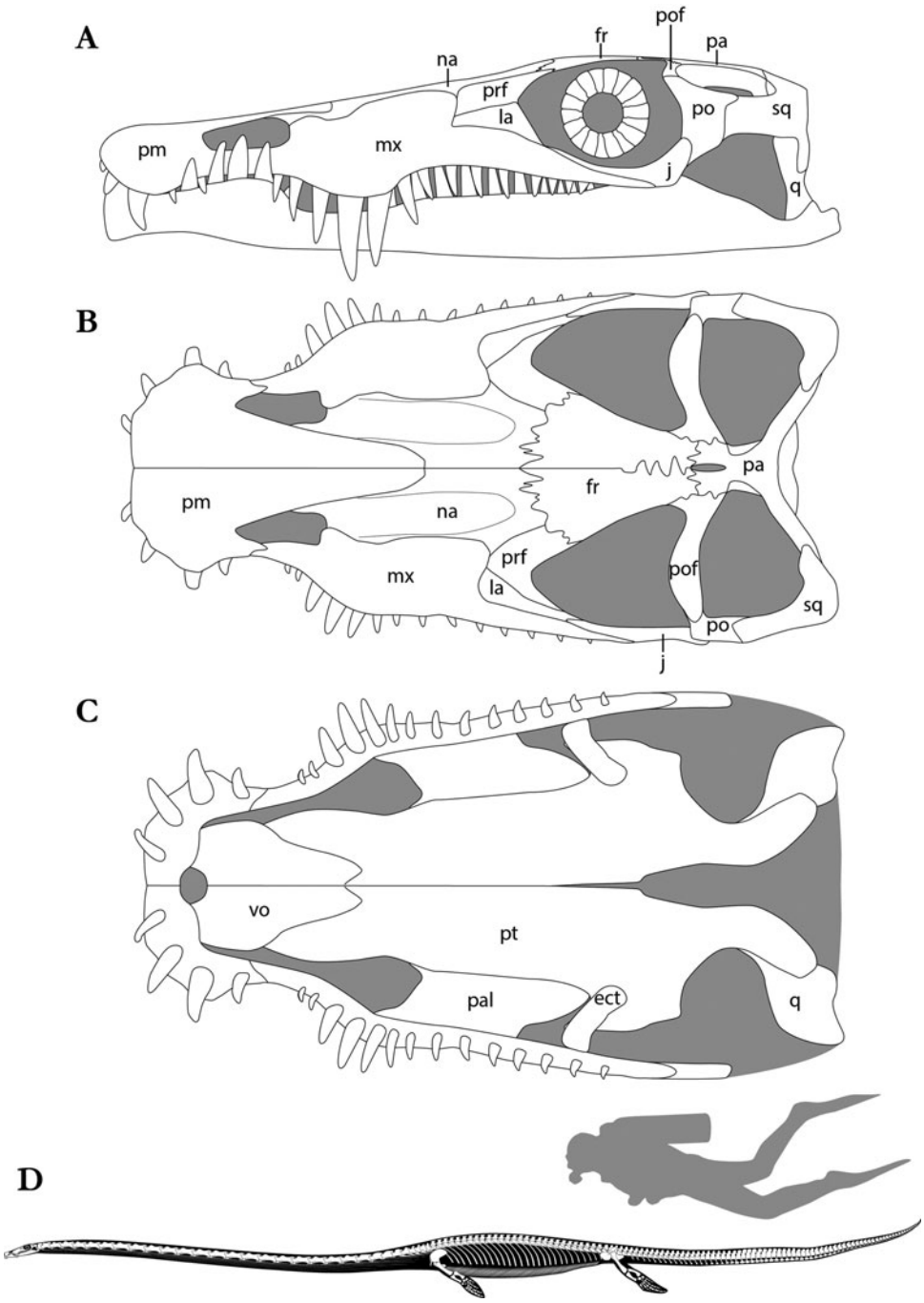

Figure 16 Restoration of *Dinocephalosaurus orientalis*. The skull in (a) left lateral; (b) dorsal; and (c) ventral views. (d) The skeleton in left lateral view with a silhouette of a diver for scale. Abbreviations; ect = ectopterygoid; fr = frontal; j = jugal; la = lacrimal; mx = maxilla; na = nasal; pa = parietal; pal = palatine; pm = premaxilla; po = postorbital; pof = postfrontal; prf = prefrontal; pt = pterygoid; q = quadrate; sq = squamosal; vo = vomer.

complete specimens, which also argues against suction feeding in this taxon. Instead, the close convergence in cranial morphology, particularly in the snout, between *Dinocephalosaurus orientalis* and *Tanystropheus hydroides* suggests a similarity in function. It was proposed that *Tanystropheus hydroides* most probably acquired its prey through a (laterally directed) snapping bite (Spiekman *et al*. 2020b), as was previously hypothesised for piscivorous Triassic sauropterygians (Rieppel 2002), and this also represents a likely hypothesis for the feeding mechanism of *Dinocephalosaurus orientalis*.

The largest specimens of *Dinocephalosaurus orientalis* clearly represent relatively mature individuals. In the holotype skull there is frequent fusion of dermatocranial elements (Fig. 1), and in IVPP V20295 and V13898 there is no separation of the neural arch from the centra in the trunk region. Furthermore, as outlined above, the gravid LPV 30280 is considerably smaller than the referred specimens of *Dinocephalosaurus orientalis*. Even though this specimen cannot be unequivocally assigned to this species, it is clearly very closely related, and thus indicative of the mature state of the *Dinocephalosaurus orientalis* specimens. Yet the limbs of the *Dinocephalosaurus orientalis* specimens are atypical for early archosauromorphs in that they are relatively short, show little development of articular surfaces, and the carpus and tarsus are very poorly ossified. Carpals and tarsals are typically developed as simple discs with no sutural contact except in the proximal carpus. Distal carpals and tarsals are sometimes missing altogether and the fifth metatarsal shows no degree of modification. By contrast, even *Tanystropheus* spp., which among all other early archosauromorphs exhibits the greatest level of paedomorphosis, retains a contact between the

https://doi.org/10.1017/S175569102400001X

astragalus and calcaneum, and the fifth metatarsal shows a proximal broadening of the ancestrally hooked fifth metatarsal. The limbs of *Tanystropheus hydroides* were thus better suited to terrestrial locomotion than those of *Dinocephalosaurus orientalis*. Bone density analysis showed the sauropterygian *Lariosaurus* to be more clearly adapted to a fully aquatic lifestyle than *Tanystropheus*, which on that basis was inferred to have been amphibious (Jaquier & Scheyer 2017). Fishing from the shoreline (Renesto 2005) has not been generally accepted as a mode of predation in *Tanystropheus hydroides* (Nosotti 2007; Jaquier & Scheyer 2017; Renesto & Saller 2018; Spiekman *et al*. 2020a, 2020b), and we consider it highly unlikely that it habitually emerged onto land: its long, straight and rigid neck making extended movement on land improbable (Tschanz 1986). If it was difficult for *Tanystropheus hydroides* to move on land then it would have been impossible for *Dinocephalosaurus orientalis*. Based on the highly elongated, serpentine body shape of *Dinocephalosaurus orientalis*, including a characteristically elongated thorax and tail, it is speculated that lateral undulation was probably the main propulsive force. Thus, *Dinocephalosaurus orientalis* is very much a serpentine-like form, whereas *Tanystropheus hydroides* is more crocodile- or varanid-like, but with a very long neck. The degree of skeletal paedomorphosis in *Dinocephalosaurus orientalis* is pronounced and indicates adaptation to life in the open water, a lifestyle that is additionally supported by the presence of vivipary in *Dinocephalosaurus* sp. and a closely related taxon (Li *et al*. 2017a; Liu *et al*. 2017). To date, all specimens of *Dinocephalosaurus* sp. have been recovered from the Upper Member of the Guanling Formation of Anisian age. Although *Tanystropheus* sp. has been recorded from eastern Tethyan deposits (Li *et al*. 2004; Rieppel *et al*. 2010), specimens occur in the younger Zhuganpo Member of the Falang Formation of latest Ladinian or earliest Carnian age. The two forms were therefore apparently not coeval, based on the currently available evidence.

4. Summary

The Middle Triassic (latest Anisian) marine reptile *Dinocephalosaurus orientalis* is fully described in detail on the basis of seven beautifully preserved specimens from southwestern Guizhou Province, southern China, five of which are presented for the first time. Characters in the skull and neck are consistent with *Dinocephalosaurus orientalis* being included within Archosauromorpha. With 32, mostly elongate, cervical vertebrae, it had an extraordinarily long neck that draws comparison with the neck of *Tanystropheus hydroides,* another aquatic non-crocopodan archosauromorph that has been recorded from the Middle Triassic of both Europe and China. Both taxa share several other cranial features, including a fish-trap type dentition, a distinct antorbital recess and a wide palatal ramus of the pterygoid. The phylogenetic placement of *Dinocephalosaurus orientalis* is hampered by high levels of homoplasy, but our analysis suggests that the similarities between *Dinocephalosaurus orientalis* and *Tanystropheus hydroides* are largely convergent. Instead, the results corroborate the presence of a monophyletic Dinocephalosauridae outside Tanystropheidae. A greater expression of paedomorphosis in the appendicular skeleton and the presence of paddle-shaped autopodia in *Dinocephalosaurus orientalis* also suggest an adaptation to more open waters than in *Tanystropheus hydroides*. *Dinocephalosaurus orientalis* and *Tanystropheus* sp. were not contemporaries in the eastern Tethys based on current fossil occurrences: all finds of *Tanystropheus* sp. to date being from latest Ladinian or earliest Carnian sequences. The exact function of the extraordinary long neck of *Dinocephalosaurus orientalis* is unclear but it almost certainly aided in catching fish, which are preserved in the stomach contents of one of the specimens.

5. Institutional abbreviations

AMNH = American Museum of Natural History, New York, NY, USA; IVPP = Institute of Vertebrate Palaeontology and Palaeoanthropology, Beijing, China; LPV = Chengdu Institute of Geology and Mineral Resources, Chengdu, China; ZMNH = Zhejiang Museum of Natural History, Hangzhou, China.

6. Supplementary material

Supplementary material is available online at https://doi.org/10.1017/S175569102400001X.

7. Acknowledgements

Shi-Xue Hu kindly provided access to the specimens of *Dinocephalosaurus* in the Chengdu Institute of Geology and Mineral Resources. The work was supported by Strategic Priority Research Program (B) of the Chinese Academy of Sciences XDB26000000. We also thank IVPP for supporting the visits of N.C.F. and O.R. to Beijing. SNFS is funded by the Deutsche Forschungsgemeinschaft (DFG project no. SCHO 791/7-1 to Rainer Schoch). We are grateful to Marlene Donnelly for the specimen line drawings and Martín Ezcurra is thanked for discussions on the use of TNT. We acknowledge the Willi Hennig Society for the free use of TNT. We also thank the Editor, Martin Ezcurra and an anonymous reviewer for their comments on the original submission.

8. Competing interests

The authors declare none.

9. References

Borsuk-Białynicka, M. & Evans, S. E. 2009. A long-necked archosauromorph from the Early Triassic of Poland. *Palaeontologia Polonica* **65**, 203–34.

Brusatte, S. L., Benton, M. J., Lloyd, G. T., Ruta, M. & Wang, S. C. 2010. Macroevolutionary patterns in the evolutionary radiation of archosaurs (Tetrapoda: Diapsida). *Earth and Environmental Science Transactions of the Royal Society of Edinburgh* **101**, 367–82.

Butler, R. J., Brusatte, S. L., Reich, M., Nesbitt, S. J., Schoch, R. R. & Hornung, J. J. 2011. The sail-backed reptile *Ctenosauriscus* from the latest Early Triassic of Germany and the timing and biogeography of the early archosaur radiation. *PLOS ONE* **6**, e25693.

Chen, X.-H., Motani, R., Cheng, L., Jiang, D.-Y. & Rieppel, O. 2014. The enigmatic marine reptile *Nanchangosaurus* from the Lower Triassic of Hubei, China and the phylogenetic affinities of Hupehsuchia. *PLOS ONE* **9**, e102361.

Dalla Vecchia, F. M. 2020. *Raibliania calligarisi* gen. n., sp. n., a new tanystropheid (Diapsida, Tanystropheidae) from the Upper Triassic (Carnian) of northeastern Italy. *Rivista Italiana di Paleontologia e Stratigrafia* **126**, 197–222.

De Oliveira, T. M., Pinheiro, F. L., Stock Da Rosa, Á. A., Dias Da Silva, S. & Kerber, L. 2020. A new archosauromorph from South America provides insights on the early diversification of tanystropheids. *PLOS ONE* **15**, e0230890.

Dilkes, D. W. 1998. The Early Triassic rhynchosaur *Mesosuchus browni* and the interrelationships of basal archosauromorph reptiles. *Philosophical Transactions of the Royal Society of London B: Biological Sciences* **353**, 501–41.

Dzik, J. & Sulej, T. 2016. An early Late Triassic long-necked reptile with a bony pectoral shield and gracile appendages. *Acta Palaeontologica Polonica* **61**, 805–23.

Ezcurra, M. D. 2016. The phylogenetic relationships of basal archosauromorphs, with an emphasis on the systematics of proterosuchian archosauriforms. *PeerJ* **4**, e1778.

Ezcurra, M. D. & Butler, R. J. 2018. The rise of the ruling reptiles and ecosystem recovery from the Permo-Triassic mass extinction. *Proceedings of the Royal Society B: Biological Sciences* **285**, 20180361.
Ezcurra, M. D., Scheyer, T. M. & Butler, R. J. 2014. The origin and early evolution of Sauria: reassessing the Permian saurian fossil record and the timing of the crocodile-lizard divergence. *PLOS ONE* **9**, e89165.
Flynn, J. J., Nesbitt, S. J., Michael Parrish, J., Ranivoharimanana, L. & Wyss, A. R. 2010. A new species of *Azendohsaurus* (Diapsida: Archosauromorpha) from the Triassic Isalo Group of southwestern Madagascar: cranium and mandible. *Palaeontology* **53**, 669–88.
Foth, C., Ezcurra, M. D., Sookias, R. B., Brusatte, S. L. & Butler, R. J. 2016. Unappreciated diversification of stem archosaurs during the Middle Triassic predated the dominance of dinosaurs. *BMC Evolutionary Biology* **16**, 188.
Fraser, N. C. & Rieppel, O. 2006. A new protorosaur (Diapsida) from the Upper Buntsandstein of the Black Forest, Germany. *Journal of Vertebrate Paleontology* **26**, 866–71.
Fraser, N. C., Rieppel, O. & Li, C. 2013. A long-snouted protorosaur from the Middle Triassic of southern China. *Journal of Vertebrate Paleontology* **33**, 1120–26.
Goloboff, P. A. & Catalano, S. A. 2016. TNT version 1.5, including a full implementation of phylogenetic morphometrics. *Cladistics* **32**, 221–38.
Gottmann-Quesada, A. & Sander, P. M. 2009. A redescription of the early archosauromorph *Protorosaurus speneri* Meyer, 1832, and its phylogenetic relationships. *Palaeontographica Abteilung A* **287**, 123–220.
Jaquier, V. P., Fraser, N. C., Furrer, H. & Scheyer, T. M. 2017. Osteology of a new specimen of *Macrocnemus* aff. *M. fuyuanensis* (Archosauromorpha, Protorosauria) from the Middle Triassic of Europe: potential implications for species recognition and paleogeography of tanystropheid protorosaurs. *Frontiers in Earth Science* **5**, https://doi.org/10.3389/feart.2017.00091.
Jaquier, V. P. & Scheyer, T. M. 2017. Bone histology of the Middle Triassic long-necked reptiles *Tanystropheus* and *Macrocnemus* (Archosauromorpha, Protorosauria). *Journal of Vertebrate Paleontology* **37**, e1296456.
Jiang, D. Y., Hao, W. C., Maisch, M. W., Matzke, A. T. & Sun, Y. L. 2005b. A basal mixosaurid ichthyosaur from the Middle Triassic of China. *Palaeontology* **48**, 869–82.
Jiang, D.-Y., Hao, W.-C., Sun, Y.-L., Maisch, M. W. & Matzke, A. T. 2003. The mixosaurid ichthyosaur *Phalarodon* from the Middle Triassic of China. *Neues Jahrbuch für Geologie und Paläontologie-Monatshefte* **11**, 656–66.
Jiang, D.-Y., Maisch, M. W., Hao, W.-C., Pfretzschner, H., Sun, Y.-L. & Sun, Z.-Y. 2005a. *Nothosaurus* sp. (Reptilia, Sauropterygia, Nothosauridae) from the Anisian (Middle Triassic) of Guizhou, southwestern China. *Neues Jahrbuch für Geologie und Paläontologie-Monatshefte* **9**, 565–76.
Jiang, D.-Y., Maisch, M. W., Hao, W.-C., Sun, Y.-L. & Sun, Z.-Y. 2006b. *Nothosaurus yangjuanensis* n. sp. (Reptilia, Sauropterygia, Nothosauridae) from the middle Anisian (Middle Triassic) of Guizhou. *Neues Jahrbuch für Geologie und Paläontologie-Monatshefte* **2006**, 257–76.
Jiang, D.-Y., Motani, R., Hao, W.-C., Rieppel, O., Sun, Y.-L., Schmitz, L. & Sun, Z.-Y. 2008. First record of Placodontoidea (Reptilia, Sauropterygia, Placodontia) from the eastern Tethys. *Journal of Vertebrate Paleontology* **28**, 904–08.
Jiang, D.-Y., Schmitz, L., Hao, W.-C. & Sun, Y.-L. 2006a. A new mixosaurid ichthyosaur from the Middle Triassic of China. *Journal of Vertebrate Paleontology* **26**, 60–69.
Jiang, D.-Y., Schmitz, L., Motani, R., Hao, W.-C. & Sun, Y.-L. 2007. The mixosaurid ichthyosaur *Phalarodon* cf. *P. fraasi* from the Middle Triassic of Guizhou Province, China. *Journal of Paleontology* **81**, 602–05.
Langer, M. C., Ezcurra, M. D., Bittencourt, J. S. & Novas, F. E. 2010. The origin and early evolution of dinosaurs. *Biological Reviews* **85**, 55–110.
Li, C. 2003. First record of protorosaurid reptile (Order Protorosauria) from the Middle Triassic of China. *Acta Geologica Sinica* **77**, 419–23.
Li, C. 2007. A juvenile *Tanystropheus* sp. (Protorosauria, Tanystropheidae) from the Middle Triassic of Guizhou, China. *Vertebrata Palasiatica* **45**, 37–42.
Li, C., Fraser, N. C., Rieppel, O., Zhao, L.-J. & Wang, L.-T. 2017a. A new diapsid from the Middle Triassic of southern China. *Journal of Paleontology* **91**, 1306–12.
Li, C., Rieppel, O. & Fraser, N. C. 2017b. Viviparity in a Triassic marine archosauromorph reptile. *Vertebrata Palasiatica* **7**, 210–17.
Li, C., Rieppel, O. & LaBarbera, M. C. 2004. A Triassic aquatic protorosaur with an extremely long neck. *Science* **305**, 1931.
Li, C., Wu, X.-C., Cheng, Y.-N., Sato, T. & Wang, L. 2006. An unusual archosaurian from the marine Triassic of China. *Naturwissenschaften* **93**, 200–06.
Liu, J., Organ, C. L., Benton, M. J., Brandley, M. C. & Aitchison, J. C. 2017. Live birth in an archosauromorph reptile. *Nature Communications* **8**, 14445.
Maxwell, E. E., Caldwell, M. W. & Lamoureux, D. O. 2011. The structure and phylogenetic distribution of amniote plicidentine. *Journal of Vertebrate Paleontology* **31**, 553–61.
Miedema, F., Spiekman, S. N. F., Fernandez, V., Reumer, J. W. F. & Scheyer, T. M. 2020. Cranial morphology of the tanystropheid *Macrocnemus bassanii* unveiled using synchrotron microtomography. *Scientific Reports* **10**, 12412.
Motani, R., Jiang, D.-Y., Tintori, A., Sun, Y.-L., Hao, W.-C., Boyd, A., Hinic-Frlog, S., Schmitz, L., Shin, J.-Y. & Sun, Z.-Y. 2008. Horizons and assemblages of Middle Triassic marine reptiles from Panxian, Guizhou, China. *Journal of Vertebrate Paleontology* **28**, 900–03.
Nesbitt, S. J. 2011. The early evolution of archosaurs: relationships and the origin of major clades. *Bulletin of the American Museum of Natural History* **352**, 1–292.
Nosotti, S. 2007. *Tanystropheus longobardicus* (Reptilia, Protorosauria): re-interpretations of the anatomy based on new specimens from the Middle Triassic of Besano (Lombardy, northern Italy). *Memorie della Società Italiana di Scienze Naturali e del Museo Civico di Storia Naturale di Milano* **35**, 1–88.
Olsen, P. E. 1979. A new aquatic eosuchian from the Newark Supergroup (Late Triassic–Early Jurassic) of North Carolina and Virginia. *Postilla* **176**, 1–14.
Osborn, H. F. 1903. The reptilian subclasses Diapsida and Synapsida and the early history of the Diaptosauria. *Memoirs of the American Museum of Natural History* **1**, 449–519.
Pinheiro, F. L., Simão-Oliveira, D. D. & Butler, R. J. 2019. Osteology of the archosauromorph *Teyujagua paradoxa* and the early evolution of the archosauriform skull. *Zoological Journal of the Linnean Society* **189**, 378–417.
Pol, D. & Escapa, I. H. 2009. Unstable taxa in cladistic analysis: identification and the assessment of relevant characters. *Cladistics* **25**, 515–27.
Pritchard, A. C., Turner, A. H., Nesbitt, S. J., Irmis, R. B. & Smith, N. D. 2015. Late Triassic tanystropheids (Reptilia, Archosauromorpha) from Northern New Mexico (Petrified Forest Member, Chinle Formation) and the biogeography, functional morphology, and evolution of Tanystropheidae. *Journal of Vertebrate Paleontology* **35**, e911186.
Renesto, S. 2005. A new specimen of *Tanystropheus* (Reptilia Protorosauria) from the Middle Triassic of Switzerland and the ecology of the genus. *Rivista Italiana di Paleontologia e Stratigrafia* **111**, 377–94.
Renesto, S. & Saller, F. 2018. Evidences for a semi aquatic life style in the Triassic diapsid reptile *Tanystropheus*. *Rivista Italiana di Paleontologia e Stratigrafia* **124**, 23–34.
Rieppel, O. 1989. The hind limb of *Macrocnemus bassani* (Nopcsa) (Reptilia, Diapsida): development and functional anatomy. *Journal of Vertebrate Paleontology* **9**, 373–87.
Rieppel, O. 1995. Fragmenta Sauropterygiana. *Neues Jahrbuch für Geologie und Paläontologie-Abhandlungen* **197**, 383–97.
Rieppel, O. 2000. Sauropterygia I: Placodontia, Pachypleurosauria, Nothosauroidea, Pistosauroidea. *Encyclopedia of Paleoherpetology* **12**, 1–134.
Rieppel, O. 2002. Feeding mechanics in Triassic stem-group sauropterygians: the anatomy of a successful invasion of Mesozoic seas. *Zoological Journal of the Linnean Society* **135**, 33–63.
Rieppel, O., Jiang, D.-Y., Fraser, N. C., Hao, W.-C., Motani, R., Sun, Y.-L. & Sun, Z.-Y. 2010. *Tanystropheus* cf. *T. longobardicus* from the early Late Triassic of Guizhou Province, southwestern China. *Journal of Vertebrate Paleontology* **30**, 1082–89.
Rieppel, O., Li, C. & Fraser, N. C. 2008. The skeletal anatomy of the Triassic protorosaur *Dinocephalosaurus orientalis*, from the Middle Triassic of Guizhou Province, southern China. *Journal of Vertebrate Paleontology* **28**, 95–110.
Scheyer, T. M., Wang, W., Li, C., Miedema, F. & Spiekman, S. N. F. 2020. Osteological re-description of *Macrocnemus fuyuanensis* (Archosauromorpha, Tanystropheidae) from the Middle Triassic of China. *Vertebrata Palasiatica* **58**, 169–87.
Sengupta, S. & Bandyopadhyay, S. 2022. The osteology of *Shringasaurus indicus*, an archosauromorph from the Middle Triassic Denwa Formation, Satpura Gondwana Basin, Central India. *Journal of Vertebrate Paleontology* **41**, e2010740.

Sennikov, A. G. 2011. New tanystropheids (Reptilia: Archosauromorpha) from the Triassic of Europe. *Paleontological Journal* **45**, 90–104.

Shang, Q.-H. 2006. A new species of *Nothosaurus* from the early Middle Triassic of Guizhou, China. *Vertebrata Palasiatica* **44**, 237–49.

Spiekman, S. N. F. 2018. A new specimen of *Prolacerta broomi* from the lower Fremouw Formation (Early Triassic) of Antarctica, its biogeographical implications and a taxonomic revision. *Scientific Reports* **8**, 17996.

Spiekman, S. N. F., Fraser, N. C. & Scheyer, T. M. 2021. A new phylogenetic hypothesis of Tanystropheidae (Diapsida, Archosauromorpha) and other 'protorosaurs', and its implications for the early evolution of stem archosaurs. *PeerJ* **9**, e11143.

Spiekman, S. N. F. & Klein, N. 2021. An enigmatic lower jaw from the Lower Muschelkalk (Anisian, Middle Triassic) of Winterswijk provides insights into dental configuration, tooth replacement and histology. *Netherlands Journal of Geosciences* **100**, e17.

Spiekman, S. N. F., Neenan, J. M., Fraser, N. C., Fernandez, V., Rieppel, O., Nosotti, S. & Scheyer, T. M. 2020a. The cranial morphology of *Tanystropheus hydroides* (Tanystropheidae, Archosauromorpha) as revealed by synchrotron microtomography. *PeerJ* **8**, e10299.

Spiekman, S. N. F., Neenan, J. M., Fraser, N. C., Fernandez, V., Rieppel, O., Nosotti, S. & Scheyer, T. M. 2020b. Aquatic habits and niche partitioning in the extraordinarily long-necked Triassic reptile. *Tanystropheus Current Biology* **30**, 3889–3895.

Spiekman, S. N. F. & Scheyer, T. M. 2019. A taxonomic revision of the genus *Tanystropheus* (Archosauromorpha, Tanystropheidae). *Palaeontologia Electronica* **22**, https://doi.org/10.26879/1038.

Spielmann, J. A., Lucas, S. G., Rinehart, L. F. & Heckert, A. B. 2008. The Late Triassic archosauromorph *Trilophosaurus*. *New Mexico Museum Natural History and Science Bulletin* **43**, 1–177.

Sun, Z.-Y., Hao, W.-C., Sun, Y.-L. & Jiang, D.-Y. 2009. The conodont genus *Nicoraella* and a new species from the Anisian of Guizhou, South China. *Neues Jahrbuch für Geologie und Paläontologie-Abhandlungen* **252**, 227–35.

Sun, Z.-Y., Sun, Y.-L., Hao, W.-C. & Jiang, D.-Y. 2006. Conodont evidence for the age of the Panxian Fauna, Guizhou, China. *Acta Geologica Sinica* **80**, 621–30.

Sun, Z., Tintori, A., Lombardo, C., Jiang, D.-Y., Hao, W., Sun, Y., Wu, F. & Rusconi, M. 2008. A new species of the genus *Colobodus* Agassiz, 1844 (Osteichthyes, Actinopterygii) from the Pelsonian (Anisian, Middle Triassic) of Guizhou, South China. *Rivista Italiana di Paleontologia e Stratigrafia* **114**, 363–76.

Tschanz, K. 1986. *Funktionelle Anatomie der Halswirbelsäule von Tanystropheus longobardicus (Bassani) aus der Trias (Anis/Ladin) des Monte San Giorgio (Tessin) auf der Basis vergleichend morphologischer Untersuchungen an der Halsmuskulatur rezenter Echsen*. PhD Thesis, Universität Zürich, Switzerland.

von Huene, F. R. 1946. Die grossen Stämme der Tetrapoden in den geologischen Zeiten. *Biologisches Zentralblatt* **65**, 268–75.

Wang, W., Spiekman, S. N. F., Zhao, L.-J., Rieppel, O., Scheyer, T. M., Fraser, N. C. & Li, C. 2023. A new long-necked archosauromorph from the Guanling Formation (Anisian, Middle Triassic) of southwestern China and its implications for neck evolution in tanystropheids. *The Anatomical Record*, https://doi.org/10.1002/ar.25216.

Wild, R. 1973. Die Triasfauna der Tessiner Kalkalpen XXII. *Tanystropheus longobardicus* (Bassani) (Neue Ergebnisse). *Schweizerische Paläontologische Abhandlungen* **95**, 1–162.

Zhang, Q.-Y., Zhou, C.-Y., Lu, T., Xie, T., Lou, X.-Y., Liu, W., Sun, Y.-Y., Huang, J.-Y. & Zhao, L.-S. 2009. A conodont-based Middle Triassic age assignment for the Luoping Biota of Yunnan, China. *Science in China Series D: Earth Sciences* **52**, 1673–78.

MS received 5 April 2023. Accepted for publication 21 December 2023